Visual Lane Analysis and Higher-order Tasks - A Concise Review -

Bok-Suk Shin, Zezhong Xu, and Reinhard Klette

All three authors are members of the *.enpeda..*
(Environment Perception and Driver Assistance)
Project at the Department of Computer Science
The University of Auckland, New Zealand

The second author is also with the Computer Science Department,
Changzhou Institute of Technology, Changzhou, China.

4 September 2013

Abstract

Lane detection, lane tracking, or lane departure warning have been the earliest components of vision-based driver assistance systems. At first (in the 1990s) they have been designed and implemented for situations defined by good viewing conditions and clear lane markings on highways. Since then, accuracy for particular situations (also for challenging conditions), robustness for a wide range of scenarios, time efficiency, and integration into higher-order tasks defines visual lane detection and tracking as a continuing research subject.

The paper reviews past and current work in computer vision that aims at real-time lane or road understanding under a comprehensive analysis perspective, for moving on to *higher-order tasks* combined with various lane analysis components, and introduces related work along four independent axes as shown in Fig. 2. This concise review provides not only summarizing definitions and statements for understanding key ideas in related work, it also presents selected details of potentially applicable methods, and shows applications for illustrating progress.

This review helps to plan future research which can benefit from given progress in visual lane analysis. It supports the understanding of newly emerging subjects which combine lane analysis with more complex road or traffic understanding issues. The review should help readers in selecting suitable methods for their own targeted scenario.

1 Introduction

Lane detection and tracking are subjects of vision-based driver assistance, safety warning systems, robotics, or autonomously driving platforms. The first systems have been designed and implemented in the 1990s, such as RALPH [109], GOLD [16], SCARF [30], MANIAC [67], or LANA [76, 77]. Lane detectors and trackers are offered in cars and trucks since the late 1990s. The 2006 paper [95] provides a review on solutions based on computer vision (as this paper does as well), and presents then in detail the lane detector VioLET. The survey [14] covers all the sensing modalities used for lane detection (e.g., also radar and LIDAR); it identifies a general work flow and discusses systematically the involved steps, but without going much into details of cited papers.

Vision-based techniques can potentially work for the widest spectrum of scenarios (compared to other sensing modalities), and are also very cost efficient with respect to the used hardware. Traffic environments are still designed for human drivers, not for autonomous driving. The design addresses very much the visual abilities of human drivers. Vision-based driver assistance is thus supported by the given traffic environments. However, the human driver combines many clues for understanding roads and traffic. Current research is typically still focused on individual components such as lane detection, lane tracking, curb detection, traffic sign recognition, road surface modeling, vehicle tracking,

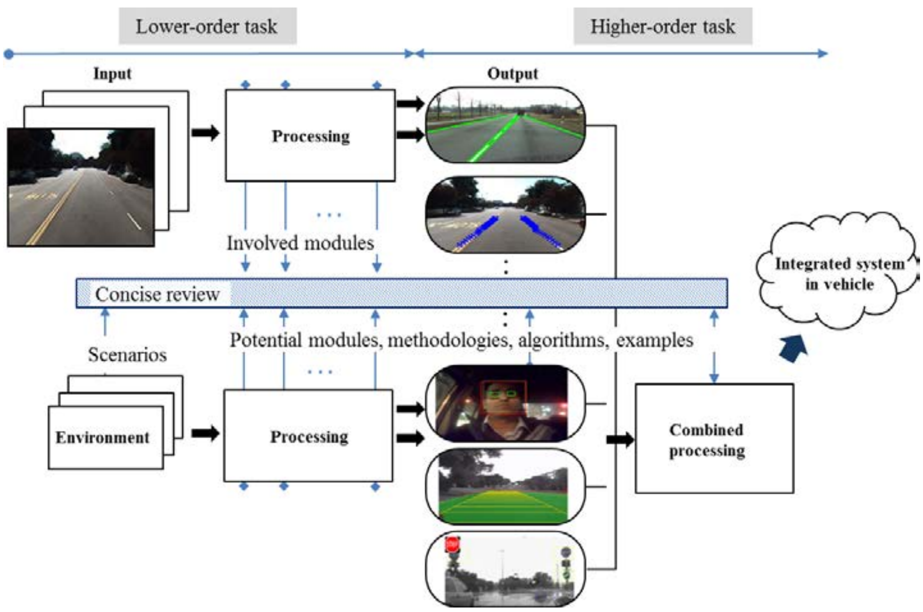

Figure 1: Framework for visual lane analysis when aiming at solutions for higher-order tasks.

pedestrian tracking, and so forth, which all contribute for a human driver to the understanding of the road environment. Future systems will integrate more individual components, using general concepts such as learning, adaptation, or model-building.

Studies on lane detection and tracking propose typically a specific method considering defined traffic scenarios, and addressing processing issues related to the proposed method, without analyzing dependencies between proposed method and considered scenarios. For instance, the reviewing papers [16, 37, 71, 95] already summarized lane models and lane analysis methodologies, but did not yet point to the different inherent complexities of scenarios, a subject which comes recently more into focus; the review in [95] contains already a table listing driving conditions (i.e. scenarios) and lane detector models.

This survey aims at presenting developments in *visual lane analysis*, i.e. subject areas which are directly related to visual lane detection and tracking. The provided references are obviously selective due to the already existing enormous number of publications, which are by far more than what could possibly be listed in such a survey. However, we were curious about the particular (new) techniques of computer vision used in visual lane analysis. We aim at providing basic definitions, and illustrate them by giving details and examples. This is one of the differences of our review to [14, 95], and we also differ by lists of discussed subjects, and by being a little more recent.

The paper is structured as follows. Section 2 provides basic definitions for lane analysis. Models for Lane Analysis are reviewed in Section 3. Section 4 discusses potential methodologies and methods with examples.

The basic tasks of visual lane analysis and lane tracking, combined with higher-order tasks, and challenges defined by applications, are dealt with in Section 5. Section 6 discusses the spectrum of scenarios aiming at characterizing particular difficulties. Section 7 concludes.

2 Visual Lane Analysis for Higher-order Tasks

After considering a wide range of proposed methods (see our bibliography), it appears to be impossible that one standardized work flow could also cover tasks of increasing complexity. A standardized work flow, as outlined in [14], is in the scope of lower-order lane analysis tasks, possibly including some hierarchical processing. The complexity and combination of higher-order tasks, combined with visual lane analysis, leads to classes of techniques incorporating learning, classification, automated model building, adaptation, and so forth.

Figure 1 indicates a framework when aiming at developing combined systems benefiting from already existing modules. Such an integration can benefit from unifying definitions or statements, key ideas or details of related work, or the current spectrum of already existing applications.

In general, *higher-order tasks* are defined by interaction with other modules in a complex driver assistance system. Examples of higher-order tasks are

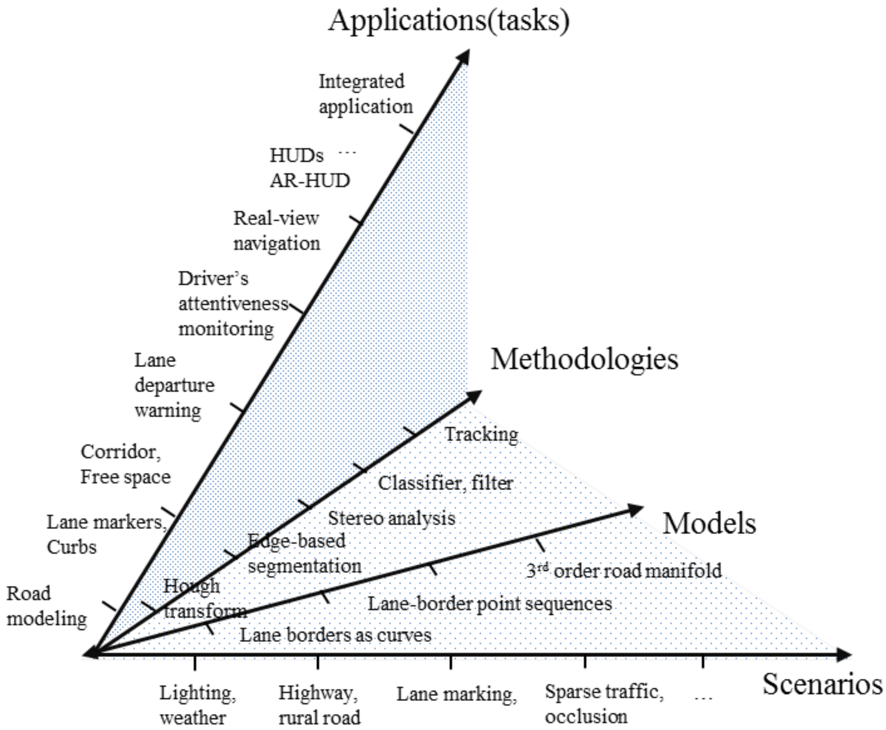

Figure 2: The scope of visual lane analysis. There are finite numbers of entries on methodology and model axes, and there is an unlimited diversity of scenarios and applications,

the combination of visual lane analysis with driver monitoring (e.g. for understanding the driver's attentiveness to the lane-keeping task [9, 48, 113]), with *ego-motion analysis* (i.e. the analysis and prediction of the trajectory of the ego-vehicle on the 2D road manifold, e.g. when calculating the lateral position of the ego-vehicle on the road), with location analysis (e.g. for improving the spatial accuracy of GPS data by identifying the position on the road), with vehicle detection [123], or with navigation (e.g. by projecting the proposed route into the real-world view of the recorded scene [49, 100, 107, 128]). Higher-order tasks are discussed in Section 5.2.

Our concise review uses independent coordinate axes for spanning a *space of proposed solutions* for visual lane analysis: the *axis of models*, the *axis of methodologies*, the *axis of applications*, and the *axis of scenarios* . See Fig. 2 for a sketch of this 4-dimensional space. Details for those axes are presented in Sections 3 to 6.

Figure 3: *Left:* single-lane roads below the historic city of Guanajuato. *Right:* unpaved two-lane road between Cachi and Cafayete.

2.1 Fundamental definitions

A *lane* L is defined by sufficient width for driving a road vehicle. It is the space between a left and a right *lane border*, being arcs γ_l and γ_r respectively. The detection of lane borders might be even a challenge for human vision due to vanishing markings, existing lane markings are covered (e.g. by parked vehicles), lighting-related issues (e.g. shadows or sunstrike), or multiple or confusing markings. Thus, we do not formalize further at this general level.

For two extreme examples of difficult lane identifications, see Fig. 3. For the shown underground road intersection, various visual clues (e.g. light in the tunnel) help to understand the geometry of the road. For a narrow two-lane road it is convenient to assume a wider lane as long as oncoming traffic is not demanding two equally-wide lanes. Note: the localization of a lane is

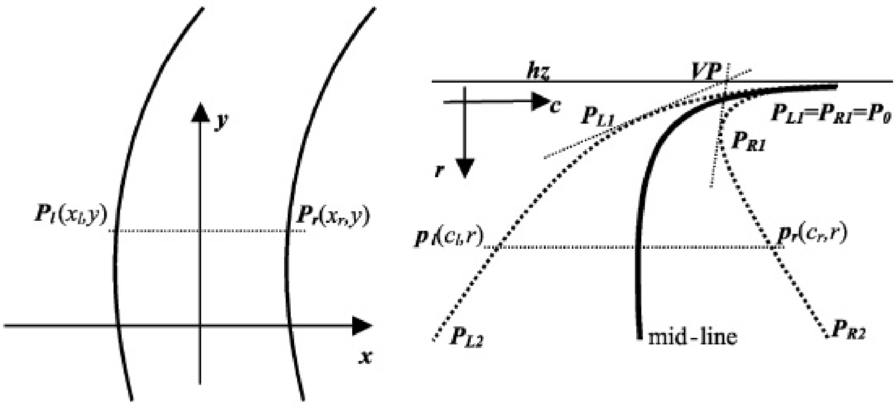

Figure 4: *Left*: bird's-eye view. *Right*: perspective view. Courtesy of the authors of [135]. Notations illustrate common coordinates in both views, with 'hz' for 'horizon' and 'VP' for 'vanishing point'.

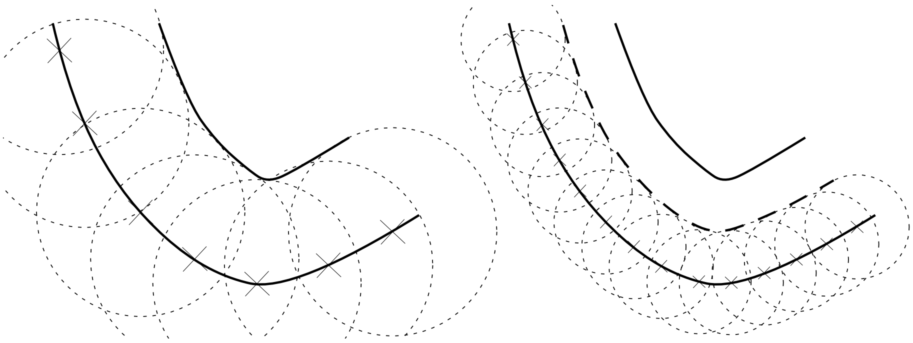

Figure 5: *Left:* parallel arcs. *Right*: parallel middle arc. A middle arc and constant width also defines the two outer parallel arcs.

not always uniquely defined in the real world; it may depend on traffic flow or driving comfort if there is no unique lane marking.

Lane analysis can be in the *perspective view* of the recorded image, or in a calculated *bird's-eye view*; see Fig. 4. A lane L is represented by a 2-dimensional (2D) smooth surface $L(u,v)$ between both borders (i.e. when not aiming at analysing unevenness of the lane), assuming some 3-dimensional (3D) XYZ Cartesian world coordinate system. Formally,

$$L(u,v) = (X(u,v), Y(u,v), Z(u,v)) \tag{1}$$

for parameters (u,v) in a 2D set, also called a *ground manifold*. In case of a planar lane, we have a *ground plane* (illustrated by the xy-coordinate system on the left of Fig. 4, thus $u = x$ and $v = y$ in this case), and one of the three coordinates in $L(u,v)$, denoting the height, is then always equal to zero.

The two borders of a lane are often assumed to be *parallel*; two arcs γ_l and γ_r are parallel if γ_l is an envelope of congruent circles (i.e. of constant radius r) centred on γ_r. Figure 5 illustrates parallel arcs for the case of a planar 2D manifold. Note that parallel arcs are *not* defined by translating one arc into the position of the other. Figure 4, left, shows translation-equivalent arcs; those two arcs are not parallel.

The *middle line* between two parallel arcs is defined by circles of radius $r/2$, if r is the radius of the circles defining the two outer parallel arcs. A lane between two parallel borders has constant *width*. Borders of roads (or lanes) are usually designed by *clothoid* segments [6, 36]. An *Euler spiral*, also known as clothoid, is an arc whose curvature changes linearly with the arc's length; using t for arc length parametrization and initial curvature $\kappa(0)$ at length $t = 0$, we have that

$$\kappa(t) = \kappa(0) + c \cdot t \tag{2}$$

for $t \geq 0$ and a defining constant $c \geq 0$. The clothoid model can represent straight lines ($\kappa(0) = c = 0$), circular arcs ($\kappa(0) > 0$ and $c = 0$), and smooth transitions between both.

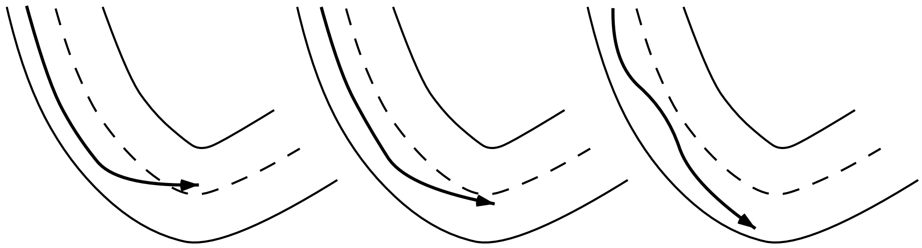

Figure 6: *Left:* lane departure. *Middle*: coming too close to the middle line. *Right*: unsteady driving.

The *ego-vehicle* is the vehicle where the system is operating in. A four-wheeled vehicle is commonly represented by the *bicycle model* [126]. For a more recent discussion of this model, see [108]. However, in this survey it is sufficient to identify the ego-vehicle with a position (i.e. a point on the road) and a direction, defining an arc by driving on a road.

Ideal *lane keeping* is defined by driving along the middle line of a lane. *Lane departure* is the crossing of one of the two lane borders. *Irregular driving* is defined by deviations from the middle line of a lane, such as, for example, coming too close to a lane border, or by unsteady driving. See Fig. 6.

2.2 Evaluation of lane analysis

Weighting the reliability of lane detection algorithms has been addressed in [15, 24]. Performance evaluation based on ground truth is discussed in [17]. See also test data with ground truth on EISATS as mentioned earlier in this paper.

The website `www.mi.auckland.ac.nz/EISATS` offers trinocular[1] rectified stereo video data (400 frames for each sequence). EISATS also provides *ground truth* (i.e. approximate truth defined by measurements or human interaction) for lane detection for those eight sequences. Trinocular data offer the possibility to evaluate the *robustness*[2] of lane detection for three monocular sequences all showing "in principle" the same scene, "just" from slightly different viewing positions.

3 Models for Visual Lane Analysis

Above we provided a 'very high-level' definition of a lane L and of its two borders γ_l and γ_r. There is no more specific formal definition of a lane due to given diversities, but a general ability of human observers to identify lanes in road images (possibly also difficulties in identifying those; compare Fig. 3).

[1] Suitable for stereo performance evaluation using the third-eye approach of [98].
[2] In general we define *robustness* by high accuracy across a defined range of scenarios.

Any formalized lane model is only an approximate representation of a particular class of geometric or visual appearances. Lane departure warning systems require an appropriate *detection range*. For example, [95] states that a minimum range of 30 meters is required to accurately predict the trajectory of the ego-vehicle in relation to detected lane borders.

Models for the *geometric shape* of a lane describe lane borders either by analytically specified curves, or by sequences of individual border points, forming some kind of irregular but 'systematic' pattern. Curves may often not match an actually irregular lane border, and when using individual points it might be difficult to initialize a border again after having it lost in a tracking process. Examples of curves are straight line segments (i.e. a linear model), or parabolic or hyperbolic arcs.

In this section we review diverse models discussed in previous work on lane analysis, addressing the axis of models in the scope of lane analysis, as shown in Fig. 2.

3.1 The linear model

The linear model appears to be appropriate for typical highway scenarios or a relatively short detection range. Short lane border segments can be approximated by straight line segments. A detection range of 30 m often already contradicts the straight segment assumption. For very precise straight lane border detection, see [142, 143].

Obviously, lane borders can always be assumed to be piecewise straight, but the length of those straight segments may often be below reasonable limits. The piecewise linear model is applied in [81, 84, 101, 146]. For non-linear lane borders, angles need to be calculated between subsequent straight segments.

3.2 Isolated points

It is also possible to model lane borders by isolated left and right border pixels in individual image rows, and to control consistency between such isolated border pixels in subsequent image rows [62, 64, 66, 149].

Example 1 *(Use of four parameters per image row): Figure 7 illustrates a model for using isolated points $P_l = (x_l, y)$ and $P_r = (x_r, y)$ as the left and right lane border points. They are identified in one image row y, defining a centre point $P_c = (x_c, y)$. Assuming a zenith point P_z at a constant height H above P_c in the real world, the zenith angle α defines points P_l and P_r. The perspective view is mapped (based on a calculated homography) into a bird's-eye view; slope angles β_1 and β_2 approximate the angles formed by the lane borders with lines in vertical direction. Altogether, four parameters $x_c, \alpha, \beta_1, \beta_2$ define the intersection of image row y with one lane. The consistency between parameter-quadruples in subsequent image rows can be controlled by a particle filter in 4-dimensional particle space. For a detailed description, see [72].*

3.3 The parabolic model and its extensions

The parabolic arc model has been commonly applied, either in the ego-vehicle coordinate system [87, 95, 97], or in the coordinate system of perspective images [83]. A parabola often fits lane marking better than the (piecewise) linear model. Obviously, it also cannot model any shape of a lane border. For example, the transition from a straight arc into a circular arc [68] is usually constructed by using a clothoid.

In [103, 124], third-order arcs are also used to model the horizontal curvature of a lane. A second-order model is deployed in [103] to model the vertical curvature of a lane. Higher-order models come with the drawback that they are more sensitive to detection noise. Temporal filtering is appropriate when using such models for robust detection. Instead of a parabolic model, some authors

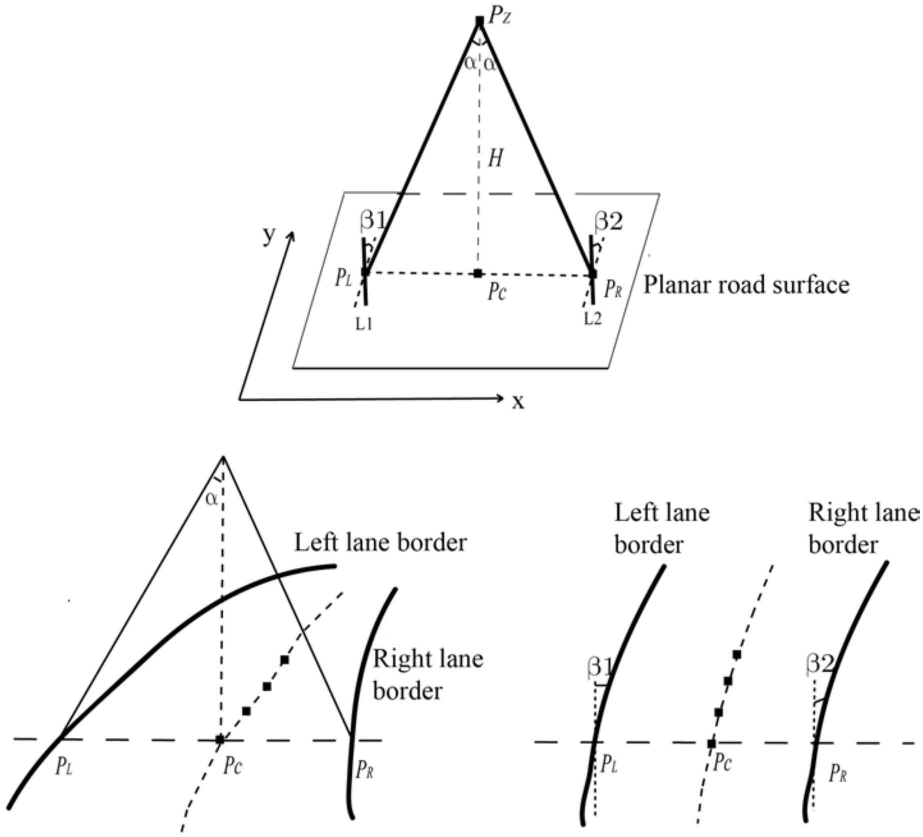

Figure 7: Lane model based on isolated points [149]. *Top*: model, assuming a planar road. *Bottom, left*: Sketch of a perspective 2D lane view in an input image. *Bottom, right*: Sketch of a bird's-eye image of the lane. See text for further explanations. Courtesy of the authors of [64].

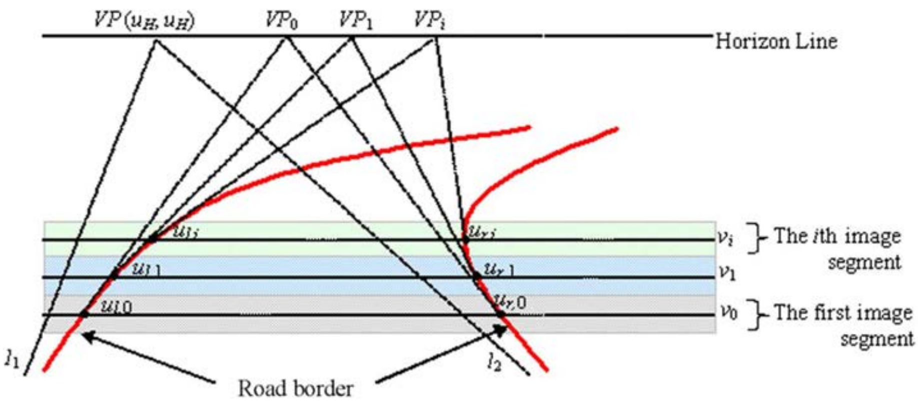

Figure 8: Hyperbolic model. Left and right lane borders are modelled by two asymptotes which define a vanishing point $VP(u_H, v_H)$ on the horizon. Courtesy of the authors of [132].

[104, 150] also use a circumference model.

3.4 Hyperbolic models

Hyperbolic arcs are considered in [77, 132] for lane shape modelling. See Fig. 8; the tangential lines l_1 and l_2 are defined by lane or road borders. The left road border is modelled by an asymptote defined by l_1 and the horizon. The right road border is similarly modelled by an asymptote defined by l_2 and the horizon. Lines l_1 and l_2 vanish at point $VP(u_H, v_H)$ on the horizon; see [132] and also [36].

3.5 Clothoid models

Segments of clothoids are used for road construction to support that only steady changes of steering angles are needed when driving from a straight into a curved road section. Clothoids have been proposed in [37] for lane or road modelling, and used in [34, 50, 78, 93].

A *clothoid road section* is defined by a sequence of constants $c_1, \ldots, c_m$ for subsequent clothoid segments of the road border.[3] When using the clothoid model for lane analysis, that constant c needs to be estimated which defines the curvature increment of the current lane section.

3.6 Spline models

Splines are piecewise polynomial curves; the connection points of polynomial segments are called *knots*, and it is commonly the goal to ensure smoothness of

[3] See Fig.7.11 in [36] for an example.

splines at knots. Splines are defined by a sequence of knots, also called *control points*, and a specified type of used polynomials. When using the spline model for lane analysis, parameters of that polynomial need to be estimated which defines the current lane border. According to [148], a spline-based lane model was first proposed in [133] using *Catmull-Rom splines* which ensure smooth changes of tangents between subsequent spline segments. In [135], the spline model was further studied by using *cubic B-splines* which are capable to describe a wider range of lane geometries.

For each frame, estimate at first the vanishing points of pairwise disjoint *regions of interest* (ROIs), then use them as control points for the calculation of B-splines. A lane is modelled as a centre line with lateral offsets. A fundamental assumption for the methods presented in [133] and [135] is that there are parallel lane markings.

In [71], a cubic spline model is used for model fitting (i.e. of a lane border). Detected pixels on lane markings are connected to form short line segments, and then fitted (based on hypotheses) using a cubic spline model and the popular RANSAC technique. Parallelism of lane markings is frequently assumed when using a spline model; see, for example, [133, 135, 150]. This assumption also helps to identify lane markings on both sides if a centre-width model is used as in [41].

3.7 Snakes

Snakes are splines defined by minimizing differences to edges or object borders in images (called *energy-minimization*). They are a common way to describe the geometric shape of 2D regions in images [69]. Snakes have been used in [135, 144] for lane border modelling. [135] uses *B-snakes* with three control points for this purpose. The assumption of parallel lane borders can be used to ensure robustness in cases of shadows, noisy image data, or missing or incorrect lane markings. Lane detection reduces here to the identification of a current set of three control points. However, in [134] it was discussed that this model "lacks the flexibility to model the complex shape of some roads."

3.8 3D models

Lane detection can also be based on 3D road models, see [102, 103, 144, 145], typically using stereo vision. The road is modelled in [103] as a 3D surface defined by horizontal, vertical curvature, lane width, and roll angle. This allows the elimination of (often simplifying) assumptions of a planar road, constant pitch angle, or any absence of a roll angle. Gradient information is used in [25] for modelling lanes; this information is useful for suppressing influences by shadows, highlights, or sun glare.

Table 1: References for Models.

Models	Features	References
Linear	Appropriate if detection range is limited, short detection range, highway scenarios.	[84, 81] [101, 146]
Isolated points	Modelling by isolated left and right border pixels, possible for irregular lane borders Control of consistency between isolated border pixels by a particle filter	[62, 64] [66, 149]
Parabolic	Fits lane marking better than the simple linear model, commonly applied	[6, 68, 83, 87] [95, 97, 103] [104, 124, 150]
Hyperbolic	Models lane shape by two asymptotes which define a vanishing point	 [36, 77, 132]
Clothoid	Supports steady changes of steering angles from a straight into a curved road section Unreliable when the road curvature tends to vary.	 [34, 50] [78, 93]
Spline	Capable to describe a wider range of lane geometries	[41, 71, 133] [135, 148, 150]
Snakes	Splines that are defined by minimizing differences to edges or object borders	[135, 144]
3D models	3D surface is defined by horizontal and vertical curvature, lane width, or roll angle. Use of stereo vision.	 [25, 102, 103] [144, 145]

4 Potential Methodologies

Used detection methodologies are typically logical conclusions of the selected model. For example, the Hough transform has been originally defined for straight segment detection and is the method-of-choice when assuming (piecewise) linear lane borders. As another example, a particle filter is an appropriate choice when using isolated points for lane borders because it allows to control control consistency between detected points in subsequent image rows.

A common strategy is to detect *candidate points* on lane borders by mapping recorded images at first from the perspective view into the bird's-eye view, and then by applying an edge filter which is trained on detecting vertical lines rather than horizontal lines. Those *vertical edge pixels* are then an input for subsequent analysis steps.

In this section, we discuss methodologies for visual lane analysis that are of potential use for more complex road or traffic scenarios, thus approaching higher-order tasks. The section addresses the axis of methodologies in the scope of lane analysis as shown in Fig. 2.

4.1 Hough transform methods

The *Hough transform* (HT) is a basic tool in image analysis for parameter estimation. It is also widely used for lane detection; see, for example, [17, 43, 44, 54, 75, 96, 114, 116, 131, 142, 147]. Image features are mapped from the image plane into the *Hough space* (also called the *accumulator array*), and the Hough space is then analysed for detecting significant clusters. Both subprocesses are suitable for parallel implementation. The original Hough transform [39] was designed for detecting straight lines in their rho-theta parameter space (as known from the Radon transform [110]):

$$\gamma : \rho = x \cos \theta + y \sin \theta \tag{3}$$

The HT was later generalized to detect arbitrary shapes mapped under some geometric transform [13]; straight segment detection is the simplest but not the only option of analysing geometric objects in a parameter space. A two-step adaptive generalized HT for the detection of non-analytic objects (under weak affine transformations) is introduced in [40]. The *statistical Hough transform* (SHT) was introduced in [31], already illustrating their use by providing a lane detection example. According to [86], the SHT overcomes shortcomings of the HT when doing lane detection.

Example 2 *(Statistical Hough transform): In contrast to the standard HT, the SHT uses all (or randomly selected) pixels and their gradients as observation data to generate a continuous probability distribution of the HT variables. At each participating pixel p, we estimate the direction θ of the image gradient (I_x, I_y) at p; this estimate and pixel location $p = (x_0, y_0)$ define a straight line $\gamma : y = m(x - x_0) + y_0$ passing through p with slope $m = I_y/I_x$. Straight line $\gamma_1 : y = -mx$ intersects γ at (x_1, y_1), and this defines $\rho = \sqrt{x_1^2 + y_1^2}$. Thus we have both parameters θ and ρ of a straight line passing through $p = (x, y)$. Now we increase the value at (θ, ρ) in the Hough space by the magnitude of the gradient at p.*

The resulting discrete non-zero accumulator values in the Hough space can then be analysed for significant clusters by using density estimations, what defines the statistical character of this transform. This might usually lead to more detected lines than actually needed. A final selection of lines can be supported by the following model: directions of left border, right border, and middle line are about equal, and the distance between left border and middle line, and between right border and middle line are also about equal.

4.2 Bird's-eye view

The mapping of the recorded perspective image into a bird's-eye view (or *top view*, or *orthogonal top-down projection*) is a common module in lane analysis techniques. It is possible to apply an *inverse perspective mapping* (IPM) based on camera calibration data [16, 18, 46, 86, 99], or to calculate simply a homography based on a mapping of four calibration marks on the road into the perspective view [65]. Left and right lane markings are almost directionally aligned in the bird's-eye view, which brings convenience for subsequent image analysis [82]. See Fig. 9, top row, for an example.

Example 3 *(Inverse perspective mapping): Assume a planar road. We map the recorded perspective view into a top-down parallel projection called the bird's-eye view. The IPM is one of the possible methods to be used. It requires the knowledge of camera intrinsic (focal length and optical centre) and extrinsic (pitch angle, yaw angle, and height above ground) parameters.*

We only consider one camera for this transform. Assume that the left-handed world coordinate system $X_w Y_w Z_w$ *is centred at the camera optical centre, and differs only by rotation from the 3D camera coordinates* X_c, Y_c, Z_c. *Pixels in the recorded image have coordinates* u *and* v, *and are at location* $(u, v, 1, 1)$ *in the camera coordinate system using homogeneous coordinates. The optical centre has coordinates* (c_u, c_v) *in the image plane. We assume focal lengths* f_u *and* f_v *in* u *and* v *direction. Axis* X_c *is assumed to be in the ground plane* $X_w Y_w$ *(i.e. there is no roll). We have pitch* α *and yaw* β, *with* $c_1 = \cos\alpha$ *and* $c_2 = \cos\beta$, *and* $s_1 = \sin\alpha$ *and* $s_2 = \sin\beta$. *Let* h *be the height of the camera's focal point above the ground plane.*

The IPM is defined by a homogeneous transformation from the image into the ground plane (i.e. the planar road). For projecting a pixel $\mathbf{p} = (u, v, 1, 1)$ *onto the road plane, apply the homogeneous transformation matrix* $\mathbf{A} =$

$$h \begin{bmatrix} -\frac{1}{f_u}c_2 & \frac{1}{f_v}s_1 s_2 & \frac{1}{f_u}c_u c_2 - \frac{1}{f_v}c_u s_1 s_2 - c_1 s_2 & 0 \\ \frac{1}{f_u}s_2 & \frac{1}{f_v}s_1 c_1 & -\frac{1}{f_u}c_u s_2 - \frac{1}{f_v}c_v s_1 c_2 - c_1 c_2 & 0 \\ 0 & \frac{1}{f_v}c_1 & -\frac{1}{f_v}c_v c_1 + s_1 & 0 \\ 0 & -\frac{1}{h f_v}c_1 & \frac{1}{h f_v}c_v c_1 - \frac{1}{h}s_1 & 0 \end{bmatrix}$$

for obtaining the point $\mathbf{Ap}$ *on the road. See, for example, [5], and also for the inverse* A^{-1} *for mapping a point* $\mathbf{P} = (x, y, -h, 1)$ *on the ground plane into a point (at subpixel accuracy) in the image plane. The IPM projects a window of interest into a bird's eye view, as shown in Fig. 9, upper row, right.*

4.3 Lane markings as ridges

Lane markings of middle lines may be understood as *ridges* (or *water sheds*) if the input image is understood as a *relief map*. See upper row of Fig. 10. This figure illustrates one way for lane marking detection in original grey-level images based on gradient information, and not based on selected candidate points. For the definition of *ridgedness*, see [92].

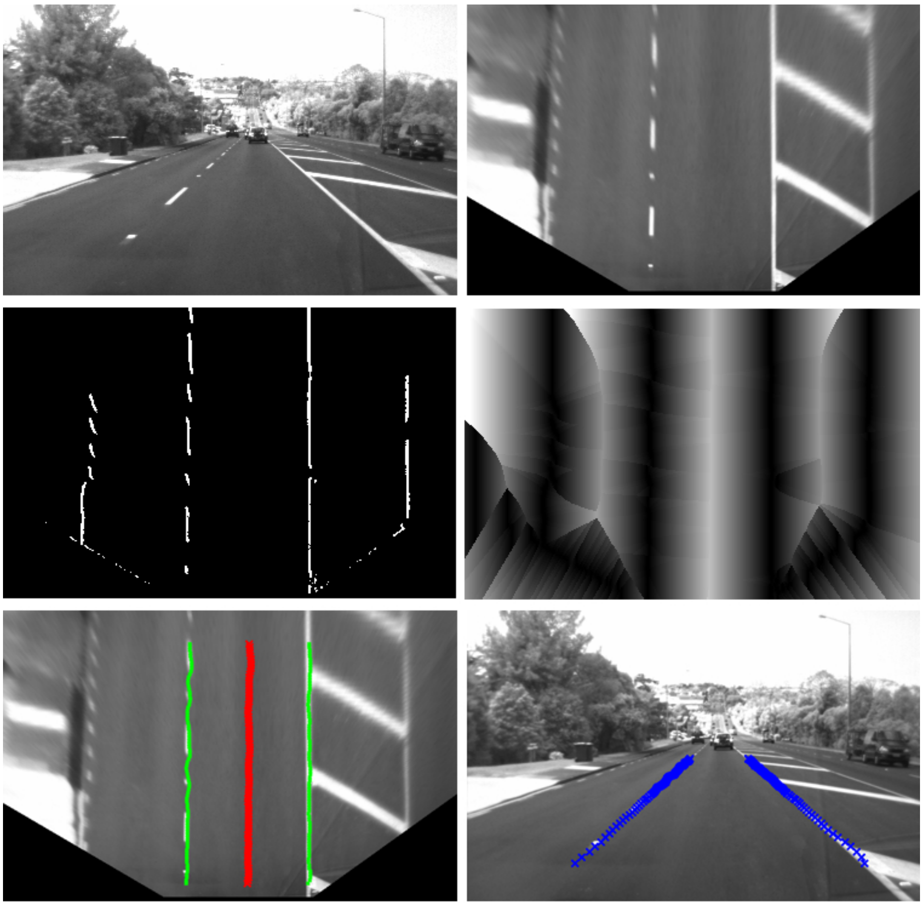

Figure 9: *Top row*: Perspective input image and bird's-eye view. *Middle row*: Edge map (i.e. detected vertical edge pixels in the bird's-eye view) and RODT map. *Bottom row*: Resulting left (green), centre (red) and right (green) pixels of the lane, and detected lane borders (blue) projected into the original input image. Courtesy of the authors of [64].

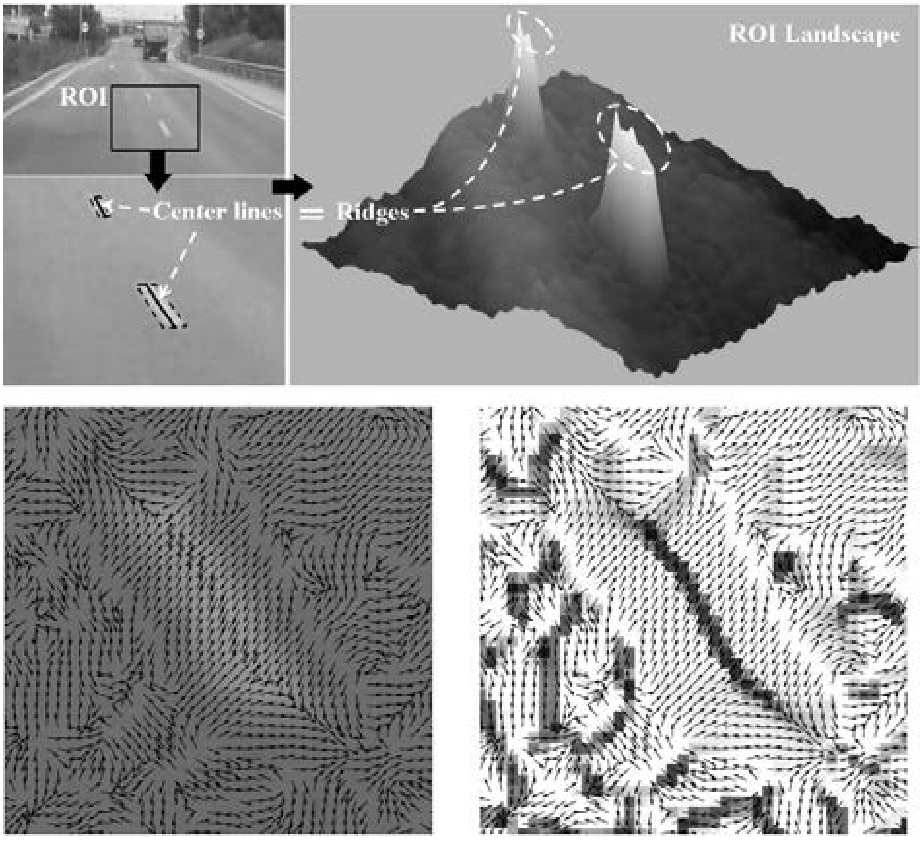

Figure 10: *Top row*: road image with outlined ROI, its magnification, and a 3D intensity visualization of the ROI in form of a relief map. *Bottom*: gradient vector field superimposed on the original image of the lower of the two lane marking segments in the ROI, and illustration of *ridgedness* for the same window. Courtesy of the authors of [92].

4.4 Euclidean distance transform

Candidate points (i.e. assumed to be in lane markings; see definition of candidate points above) can be analysed by using geometric algorithms. The *distance transform* (DT) assigns to each image pixel its shortest distance (depending on the chosen distance measure) to defined ROIs; in case the ROIs are the sets of selected candidate points. It is a fundamental geometrical operator with great applicability in computer vision and graphics, shape analysis, pattern recognition, or computational geometry; see, for example, [42, 74]. The use of the Euclidean distance measure

$$d_e(p,q) = \sqrt{(x_p - x_q)^2 + (y_p - y_q)^2} \tag{4}$$

defines the *Euclidean distance transform* (EDT) on digital images, which can be efficiently calculated; [45] showed that a 2D EDT can be performed by only calculating two 1-dimensional EDTs. The EDT is a valuable tool for lane detection [32].

For any pixel p of a given binary image I (representing the candidate points q by $I(q) = 1$), the EDT determines a value of a *distance map* D as follows:

$$D(p) = \min\{d_e(p,q) : q \text{ pixel in } I \ \wedge\ I(q) = 1\} \tag{5}$$

Candidate points are obviously labelled by value 0; in a visualization of the distance map they are shown as black pixels. Pixels p far away from object pixels have large values $D(p)$ and are shown in grey to white, where white encodes the maximum distance.

Example 4 *(Use of the RODT for detecting the centre of a lane): Let the ROIs be the selected candidate points (i.e. vertical edge pixels), and we assume a binary edge map I as input, with $I(p) = 1$ if and only if pixel p is a candidate point. The EDT specifies the shortest Euclidean distance to any candidate point.*

Now consider a modified EDT as proposed in [141], called orientation distance transform (ODT). The Euclidean distance in Equ. (4) possesses two contributing components $x_p - x_q$ and $y_p - y_q$ in row and column direction, respectively, and the ODT assigns these two components to a pixel p rather than a final result $D(p)$.

The row component RODT of the ODT labels each pixel only with the row distance value to the nearest edge pixel. Moreover, these RODT values are signed, with a positive value indicating that the nearest candidate point lies to the right, and a negative value if it is to the left. Figure 9 illustrates in the middle row the binary image of candidate points and the RODT map showing absolute RODT values in grey levels. The RODT offers a way to identify the centre of a lane being a place where negative and positive RODT values meet. The absolute value of the RODT value is also expected to be a local maximum at the centre of a lane. A local maximum in an expected range of values can be used to initialize lane border pixels in one image row, either for arcs starting in this row or for a pattern (i.e. a set of points satisfying some kind of consistency constraint) of isolated points in subsequent image rows.

The DT is sensitive to noise in input images. Thus, it is recommended to apply a denoising method on input images prior to a DT.

4.5 Stereo analysis

Lane analysis often still assumes a restriction on monocular video data, but there is an increasing interest in the use of stereo data information. Real-world data come with brightness differences between left and right views. The use of edge maps as input data for stereo matchers rather than of the original input images has been proposed in [53] for resolving the brightness difference problem. Later on, residuals with respect to smoothing proved to be an even better preprocessing method [129]. Another option is to use (in the stereo matcher) data cost functions which are insensitive to brightness variations, such as the census cost function [56]. The outcome of the *Robust Vision Challenge* at ECCV 2012, using a HIC dataset,[4] illustrated that stereo analysis is today already 'fairly robust' even for challenging scenarios defined by events such as rain, sunstrike, or night; the winning program iSGM is described in [57]. See Figure 11 for an illustration of calculated (and colour-coded) depth- or disparity maps.

Available disparity or depth data can then be used for estimating the ground manifold, for example by calculating lower envelops of summarized vertical disparities [117], or for analysing the road geometry for further features (e.g. curbs or bumps), which will be discussed later in the paper.

Example 5 *(iSGM): Semi-global matching (SGM), see [58], is one of the most successful stereo-analysis strategies currently. Iterative SGM (iSGM), see [57], refines the basic SGM strategy by (a) translating the parallel integration strategy of SGM into an iterative scheme, (b) introducing a novel data structure, the semi-global distance map (SGDM), which can be employed for effective spatial evaluation, and (c) the use of SGDMs to iteratively reduce the search space by locking reliable disparities from a pre-evaluated disparity prior.*

Horizontally accumulated costs are given a higher weight, which stabilizes recovering road surfaces. This is especially true for challenging stereo data (e.g. in the rain), as illustrated by Fig. 12.

4.6 Classifiers and filters

Data extracted for lane analysis are often also processed by a selected classifier. For example, [70] proposes a probabilistic grouping of detected lane border elements. [80] uses a Bayes pixel classifier for two features, lane colour and edge direction, and PDFs are estimated for both features by adapting to road conditions. Fuzzy C-mean and fuzzy-rules are defined in [130] for detecting edges

[4] See hci.iwr.uni-heidelberg.de/Static/challenge2012/.

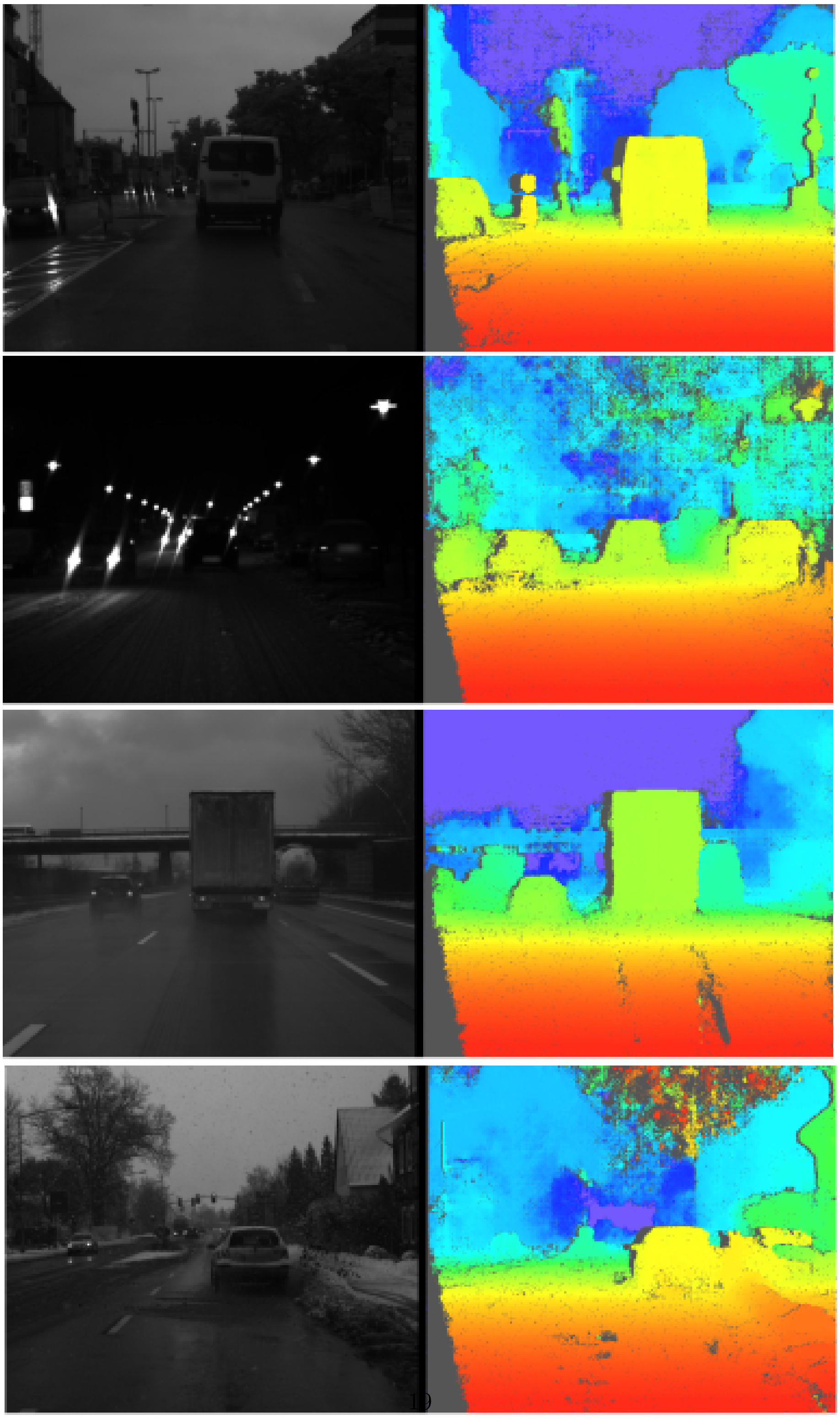

Figure 11: *Left column*: Examples of input images from the ECCV 2012 Robust Vision Challenge. *Right column*: Colour-coded depth maps calculated with iSGM [57]. Courtesy of Simon Hermann.

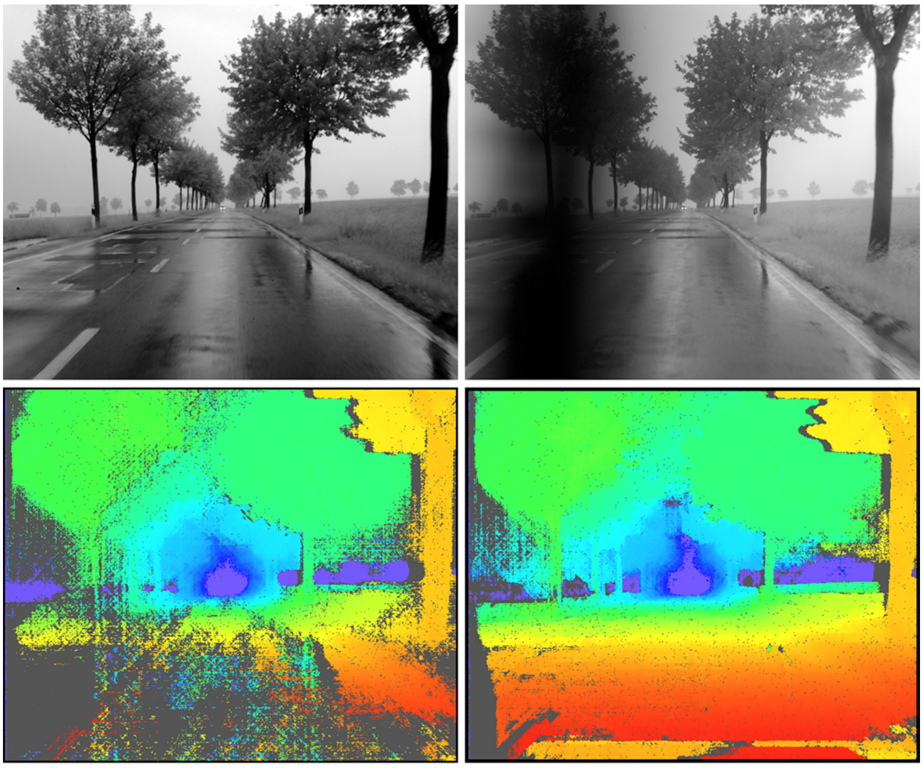

Figure 12: *Top row*: Stereo pair from the from the HIC dataset showing an ally road on a rainy day. *Bottom row*: Disparity maps when using standard SGM (left) or iSGM (right). Courtesy of the authors of [57].

within a lane detection system Particle filters [33, 71, 82, 85, 86] or Kalman filters [90] are common tools for lane tracking solutions.

Example 6 *(Use of particle filter for lane detection): The state vector* $X = (x_c, \alpha, \beta_1, \beta_2)^T$ *is defined by the parameters of the lane model (see Example 1 and Fig. 7), without* y_c*, as* y_c *will be calculated incrementally by applying a fixed step* Δ*, starting at a chosen row* y_{c_0} *in the bird's-eye image. For re-sampling, an observation model is used which determines each particle's importance factor. Based on the RODT information, it is reasonable to assume that points on lane borders (i.e. close to detected edges) have small distance values, while those on the centre of a lane (i.e. no detected edge nearby) have large distance values. In terms of the used lane model, points* (x_{c_n}, y_{c_n}) *have large distance values, and* L_1 *and* L_2 *coincide with short lines of pixels which all have small distance values. Tracking step* n *is identified by* $y_{c_n} = (y_{c_0} + n \cdot \Delta)$*. It calculates the lateral position of the left border point of the lane from the predicted state vectors, with* $\hat{X}^i_n(\hat{x}^i_{c_n}, \hat{\alpha}^i_n, \hat{\beta}^i_{1_n}, \hat{\beta}^i_{2_n})$ *for the* i^{th} *particle.*

P_l *and* P_r *only represent the lateral position of border points, for simplicity. The left position is calculated as follows:*

$$P^i_l = \hat{x}^i_{c_n} - H \cdot \tan \hat{\alpha}^i_n \tag{6}$$

Next, the sum $S^i_{L_1}$ *of the distance values along line segment* L_1 *equals*

$$\sum_{j=-L_1/2}^{L_1/2} \left| d\left(P^i_L + j \sin \hat{\beta}^i_{1_n},\, y_{c_n} + j \cos \hat{\beta}^i_{2_n}\right) \right| \tag{7}$$

Here, $d(\cdot,\cdot)$ *is the signed distance value from the RODT.* $S^i_{L_2}$ *can be calculated in an analogous way. The distance value for the centre point* $(x^i_{c_n}, y_{c_n})$ *equals* $d(x^i_{c_n}, y_{c_n})$*. Finally, RODT-based importance factors of particles can be calculated from* $S^i_{L_1}$*,* $S^i_{L_2}$*, and* $d(x^i_{c_n}, y_{c_n})$*.*

4.7 Lane tracking

Lane *tracking* is defined by a sequence of repeated detections; it is appropriate to use information from previous detection results to facilitate the current detection. Actually, there are two aims when utilizing previous information, namely to improve the computation efficiency as well as the accuracy of the current detection; continued accuracy defines robustness.

The level of achieving efficiency and robustness at the same time depends on the complexity of a given scenario. Defined mechanisms for propagating detection results may slow down the process, or lead to inaccurate results. Lane detection in some situations (e.g. on a highway) is easier compared to others (e.g. on an urban road), depending on road conditions and the quality of lane marks. In conclusion, when performing lane tracking, it is possible to pay more attention to computation efficiency for less challenging situations, but more

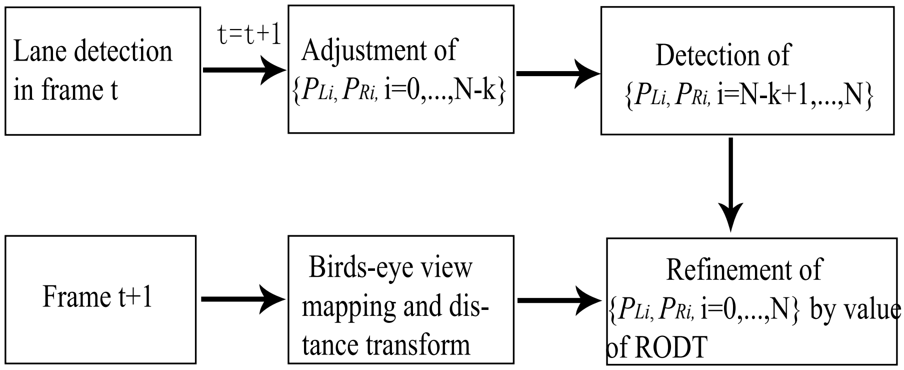

Figure 13: A possible efficient lane tracking scheme when using isolated points and RODTs as in Example 4: Left- and right lane border points in uppermost $N-k+1$ image rows at time t are used as initial values for lowermost $N-k+1$ image rows at time $t+1$; the value of k is defined by ego-motion. Courtesy of the authors of [64].

attention to robustness for challenging situations. Thus, we may classify lane tracking methods into categories of being *efficient* (for simpler scenarios) or *robust* (for a larger variety of scenarios).

4.7.1 Efficient lane tracking

Efficient lane tracking methods are designed for situations characterized by good road conditions and a good quality of lane marks (such as on a highway). In such situations, some of the previously detected lane border points can be repositioned in the image due to estimated *ego-motion* (i.e. the motion of the ego-vehicle), and then used as priors for a 'quick' refinement process due to the actual data in the image at time $t+1$. See Figure 13 for a graphical sketch of such an approach. If arcs are used for lane modelling, then tracking can also be performed by "tracking curves in dense visual clutter" [60], leading to interesting problems in computational geometry.

Example 7 *(Efficient lane tracking when using isolated points): When a lane is described by isolated points, as described in Example 1, its location is represented by two sequences* $\{P_{L_n} : n = 0, 1, \ldots, N\}$ *and* $\{P_{R_n} : n = 0, 1, \ldots, N\}$ *of points on its left and right lane border in the bird's-eye image (or similarly, by those points mapped back into the original image). The value of* N *is determined by the desired forward-looking distance. The tracking of a lane through a recorded image sequence is then simplified as tracking of such two sequences of points. The location defined by sequences* $\{P^{(t)}_{L_n}\}$ *and* $\{P^{(t)}_{R_n}\}$ *at time* t *are* *already partially driven through by the ego-vehicle at time $t + 1$, depending on its ego-motion, to be determined by available sensors and/or visual odometry. The detection process of $\{P_{L_n}^{(t+1)}\}$ and $\{P_{R_n}^{(t+1)}\}$ at time $t + 1$ may be composed of three steps: (1) adjustment of points detected at time t due to ego-motion, (2) detection of new points, and (3) refinement of point localization according to values of the RODT for the bird's-eye edge map. For example, in [62, 64, 66] this was detailed as follows: assuming a straight move from t to $t + 1$, we have that*

$$P_{L_n}^{(t+1)} = P_{L_{(n+k)}}^{(t)}, \qquad P_{R_n}^{(t+1)} = P_{R_{(n+k)}}^{(t)} \tag{8}$$

for $n = 0, 1, \ldots, N - k$, where k is determined by the driven distance between t and $t + 1$. Because k is typically small, only a few new points

$$\{P_{L_n}^{(t+1)}, P_{R_n}^{(t+1)} : n = N - k + 1, \ldots, N\}$$

need to be detected. For example, assuming smoothness of lane borders we can simply initialize for $n = N - k + 1, \ldots, N$ as follows:

$$P_{L_n}^{(t+1)} = P_{L_n}^{(t+1)}, \qquad P_{R_n}^{(t+1)} = P_{R_n}^{(t+1)} \tag{9}$$

In a concluding refinement step, those initial predictions $\{P_{L_n}^{(t+1)}\}$ and $\{P_{R_n}^{(t+1)}\}$ need to be adjusted due to the actual image data in frame $t + 1$. For example, simply by shifts in x-coordinates by

$$d(P_{L_n}^{(t+1)}, y_{c_n}) \quad \textit{and} \quad d(P_{R_n}^{(t+1)}, y_{c_n}) \tag{10}$$

for all the $N + 1$ points, where d is short for RODT values of the current bird's-eye edge map.

Efficient lane tracking schemes are designed for speed without reducing accuracy for the scenarios they are designed for. The technique in the given example above works well on highway-like situations because there are only minor variations expected between subsequent frames. However, outliers occur caused by some noisy non-border edge points, possibly removed by a higher-level control mechanism (e.g. to aim at smooth lane borders).

4.7.2 Robust lane tracking

Urban roads differ from highways by an increased complexity of environments which are possibly of relevance for accurate lane detection. In such situations, the focus shifts on robustness [8, 61, 71]. Robust lane tracking can continue to utilize (potentially) detection results from previous frames up to time t, but needs to investigate more closely for the current frame $t + 1$ for deriving a possible alternative for detection results. Occlusions are one of the problems for lane tracking, and [140] discusses way to resolve related issues.

Figure 14 illustrates the use of three potential alternatives within an isolated-points approach as illustrated by Example 4. A maximum-likelihood comparison

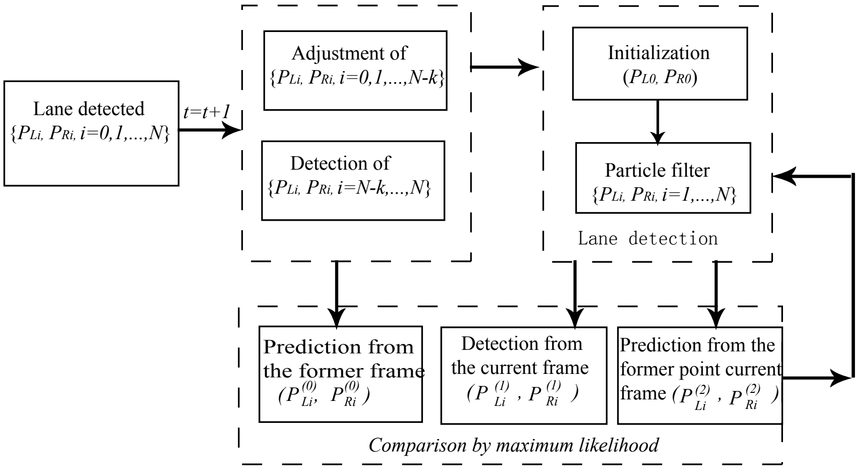

Figure 14: Robust lane tracking when using isolated points and RODTs as in Example 4. Courtesy of the authors of [64].

is used to decide for one of the three alternatives. Obviously, this costs more time compared to the design model of efficient tracking, but aims at a more careful analysis at time $t+1$. Robust lane tracking can also be performed at selected time slots $t+\triangle t$, $t+2\triangle t$, ... only, for some value $\triangle t > 1$, with efficient lane tracking in between.

Example 8 *(Robust lane tracking when using isolated points) This process is described as an extension of Example 7, and illustrated in Figure 14. Multiple alternatives are considered at time $t+1$, thus aiming at selecting the best possible match with the actually recorded frame at time $t+1$. For example, in [62, 64, 66] this was detailed as follows:*

For the first alternative $\left(P^1_{L_n}, P^1_{R_n}\right)$, we do as in efficient lane tracking, but introduce a control mechanism to prevent lane border points from diverging (e.g. caused by imperfect road conditions); for example, differences between subsequent x-coordinates can be limited by a threshold.

For the second alternative $\left(P^2_{L_n}, P^2_{R_n}\right)$, we perform lane detection as described in Example 4, that means we consider frame $t+1$ as being independent of frame t, initialize the four parameters $x_c, \alpha, \beta_1, \beta_2$ (i.e. one particle) for one row, and propagate those values bottom-up, row by row, by selecting the four parameters in the next row using a particle filter.

For the third alternative $\left(P^3_{l_n}, P^3_{r_n}\right)$, we project previous points at time t into the frame at time $t+1$ (according to ego-motion) and optimize the location of an initialized point in row y by applying a particle filter for this row (e.g. by selecting randomly more candidates 'nearby'), very similar to the bottom-up *approach for the second alternative.*

Those three alternatives are then compared using a maximum-likelihood approach based on a likelihood function $p(z|k)$*, with* z *for observed features and the* k^{th} *alternative, for* $k = 1, 2, 3$*. Value* $p(z|k)$ *denotes the probability of observing a lane border correctly by alternative* k *when considering features* z*, with the maximum likelihood estimation written as follows:*

$$P^* = arg \max_{k=1,2,3} p(z|k) \tag{11}$$

For specifying the likelihood function $p(z|k)$*, we may derive information about the width of the lane, and use RODT values.*

For estimating the width of the lane for frame $t + 1$*, we assume a Gaussian distribution with mean* W *(defined by the mean width of the lane in frame* t*) and variance* aW*, for* $0 < a < 1$*; for* $k = 1, 2, 3$ *we have that*

$$p^k_{width} = \frac{1}{aW\sqrt{2\pi}} \exp(-\frac{(P^k_{r_n} - P^k_{l_n} - W)^2}{2a^2W^2}) \tag{12}$$

We may use RODT values to evaluate the possibility that $k = 1, 2, 3$ *detects correctly lane borders:*

$$p^k_{rodt} = b \exp(-c \cdot (d(P^k_{r_n}) + d(P^k_{l_n}))^2) \tag{13}$$

where constants $b > 0$ *and* $c > 0$ *are determined by the importance ratio between* p_{width} *and* p_{rodt}*. (For example,* $b_2 = 1$ *and* $c_2 = 0.001$*.) The final value of the likelihood function can be calculated by*

$$p(z|k) = p^k_{width} \cdot p^k_{rodt}, \qquad k = 1, 2, 3 \tag{14}$$

The comparison of $p(z|k = 1)$*,* $p(z|k = 2)$*, and* $p(z|k = 3)$ *selects the alternative with the largest likelihood value as being the final detection result in the* n^{th} *row of the input image at time* $t + 1$*.*

5 Tasks and Applications

Road environments need to be understood with respect to the road surface (planar, slope of some percentage of increase or decrease), road features such as curbs or drawn markers (pedestrian crossing, writing on the road, and so forth), and, complex road geometries at intersections, roundabouts, exits of highways, and so forth. Lane detection and tracking is an important component for obtaining meaningful results in those areas.

The road environment of the ego-vehicle is analysed for different tasks, such as updating permanently the potential space for "escape routes" in case of a suddenly detected danger for human safety, informing about lane departure,

Table 2: References for methodologies.

Methodologies/Examples	Features	References
Hough transform/ Statistical Hough transform: Example 2	Detection of straight lines or of arbitrarily parametrized shapes. Contribute to the lane hypothesis. Run-time optimization proposals	 [17, 31, 43, 44] [54, 75, 96, 116] [131, 142, 143, 147]
Bird's-eye view/ Inverse perspective mapping: Example 3	Mapping of recorded perspective view into orthogonal top-down projection	[16, 18, 46] [64, 65, 82] [86, 99]
Euclidean distance transform/ RODT: Example 4	Using fundamental geometric operator with applicability Row-component only.	 [32, 42, 45] [64, 74]
Stereo analysis/ Semi-global matching: Example 5	Solutions by using distance data Suitable for real-time driver assistance Designed for challenging scenarios.	[51, 53, 56] [57, 58]
Classifiers and filters/ Particle filter:example 6	Process a probabilistic grouping of detected lane border elements	 [33, 64, 71] [82, 85, 86]
Lane tracking/ Efficient,Robust lane tracking: Example 7, 8	Computationally efficient and robust for complex road scenarios	 [8, 60, 61] [62, 64, 66] [71]

or for projecting proposed navigation routes into the real-world video data, correctly onto the lanes available for driving.

This section discusses lower-order tasks which are basic components for higher-order tasks, and higher-order applications which combine multiple modules or approaches. The section addresses the axis of applications in the scope of lane analysis as shown in Fig. 2.

5.1 Lower-order tasks

Identifying and tracking lanes in recorded video data is *the* basic task in visual lane analysis. Examples of subsequent *lower-order tasks* (i.e. not addressing other modules of driver assistance) are the detection of lane departure or of irregular driving, the estimation of the 2D manifold $L(u, v)$ of the road ahead, or of the *free space* where the ego-vehicle can navigate without any collision [11].

5.1.1 Road modelling

Roads (or lanes) are detected as surfaces (or *manifolds*) in 3D space in [91]. *Road shape* is defined in [124] by geometric features. Figure 15 shows a change in road curvature of a winding road using a B-spline road surface model.

Road surfaces are often approximated by using lower envelops of v-disparity maps [55, 79]. [117] proposes a region growing method for vertical road modelling, which iteratively performs a least-square fit of a B-spline to a region of selected points; experiments show that this method outperforms two techniques based on v-disparity maps only.

A special subject is the presence of windscreen wipers [118] which partially obstruct the view of the used cameras. Figure 16 illustrates the comparative use of three stereo matchers for detecting road surfaces. The used matchers are semi-global matching (SGM) and graph cut (GC), both using a census cost function, and belief propagation (BP) using a gradient end-point error cost function. A wiper is visible in the left image. The wiper can only be seen by one camera, and it is thus impossible to find any matching pixel pairs for the image region it covers. Stereo matchers respond differently to this situation.

Figure 15: Calculated 3D road surface of one lane using a B-Spline-based manifold model. Courtesy of the authors of [91].

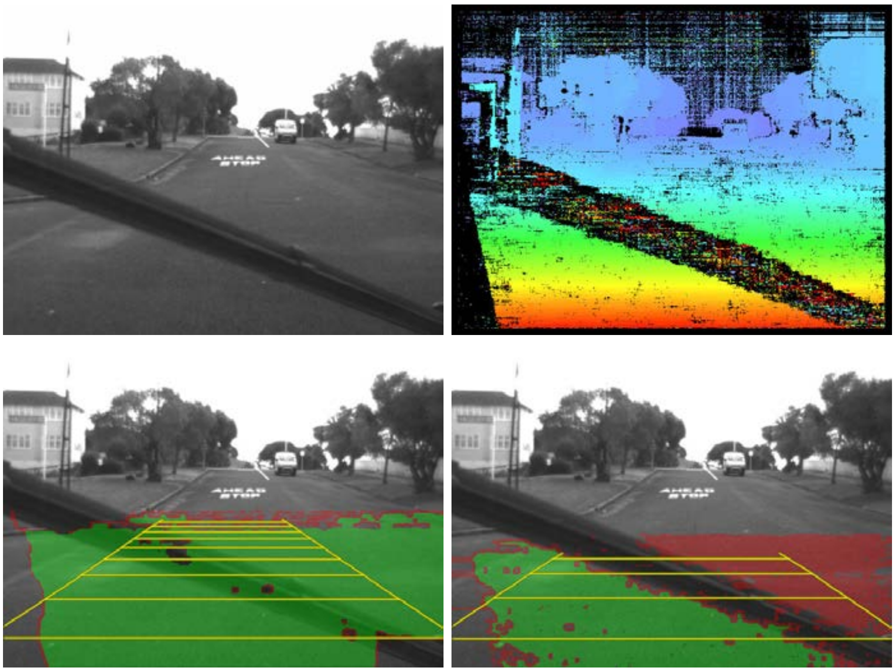

Figure 16: Input image with windscreen wiper, example of a depth map when using SGM stereo analysis, detected road surface using a BP stereo matcher. and detected road surface using a GC stereo matcher. Courtesy of the authors of [118].

5.1.2 Lane markers

[5] detects lane markers in bird's-eye views of urban streets by fitting Bezier splines to detected lines, aiming at being robust and time efficient. [12] detects lane markers following a similar approach using detected edges and segments for understanding lane markers. The detection of pedestrian crossings is discussed in [89].

[23] provides a general introduction into road mark detection and the importance of discussing driver monitoring and road understanding as a connected subject. [22, 27] detect on-road markers such as lane, pedestrian crossings, speed bumps, and stop lines for the autonomous vehicles.

5.1.3 Curbs

Curbs are modelled in [106] as straight or curved driving area delimiters. Dense stereo vision is used in [105] for curb detection, based on a created *digital elevation map* (DEM) for the road environment ahead of the ego-vehicle. Conditional random fields are used in [122] for curb reconstruction. Results indicate that the approach is able to deal with curbs of different curvature and varying height. See Fig. 17.

[121] contains a temporal filter approach for real-time curb detection and reconstruction. The paper conclude an ability of the proposed method to yield accurate reconstruction results up to a distance of 20 m to the camera. Regarding limitations it is stated that curbs violating the used assumption too much (such as those of small traffic isles) cannot be reconstructed. [139] uses LIDAR data for curb detection.

5.1.4 Corridor

Paper [63] defines a *corridor* as a "constant-width road patch ahead that will be driven through 'shortly', with constraints from physical lane borders as well as driving direction and the lateral position of the ego-vehicle". See Figure 18 for an illustration. The width $w + \varepsilon$ of the corridor is defined by the known width w of the ego-vehicle and some *safety increment* $\varepsilon > 0$.

The calculation of corridors not only requires single or multiple lane detections but also an understanding of the trajectory of the ego-vehicle (to be derived from motion sensors or visual odometry), and of obstacles ahead (derived from stereo vision or other sensors), see [65].

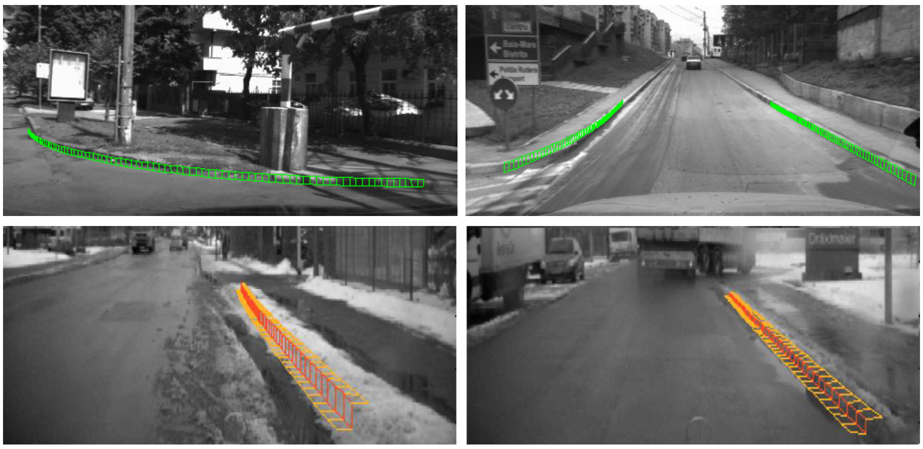

Figure 17: *Top*: Results of the proposed polynomial curb detection algorithm in [105]. The figure on the right shows a 10 % uphill road. Courtesy of the authors of [105]. *Bottom*: Reconstruction results of scenes with curbs covered by snow. Although there is no sharp height discontinuity at the curbs, the actual lane border is estimated with good accuracy. Courtesy of the authors of [122].

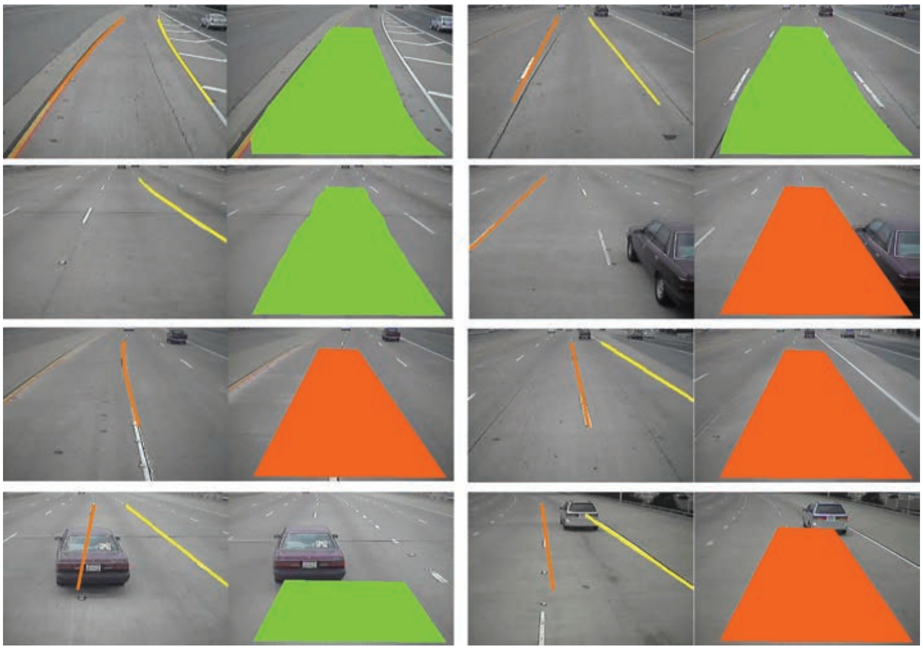

Figure 18: A comparison of detected lanes and corridors. The corridors are shown as green or red regions; 'red' indicates a detected lane change. Corridors are limited by obstacles. Courtesy of the authors of [63].

5.1.5 Free space

The *free space* is defined to be a connected region adjacent to the position of the ego-vehicle "where navigation without collision is guaranteed" [11]. See Fig. 19. The authors of [11] use the model of an *occupancy grid* (a 2D array for the bird's eye view which models occupancy evidence), where *occupancy* is defined by having an obstacle within a cell of this grid, assuming a planar road environment and only obstacles of positive height.[5] Kalman filtering is used to improve the stereo analysis results on recorded video data when analysing for obstacles.

Obviously, free space detection is a permanent task for autonomously driving vehicles. See, for example, [27] for a multi-sensor approach (also using LIDARs) for *environment detection and mapping*, also known as *simultaneous localization and mapping* (SLAM). [139] uses LIDAR data only for lane detection.

[137, 138] uses stereo vision for modelling road surfaces by B-splines, applies then a road-obstacle segmentation algorithm for deriving the free space. Figure 19 illustrates with in the middle that a planar ground manifold assumption is invalid in the depicted scene, and that it yields errors in free-space estima-

[5] The occupancy grid is called 'evidence grid' in [90].

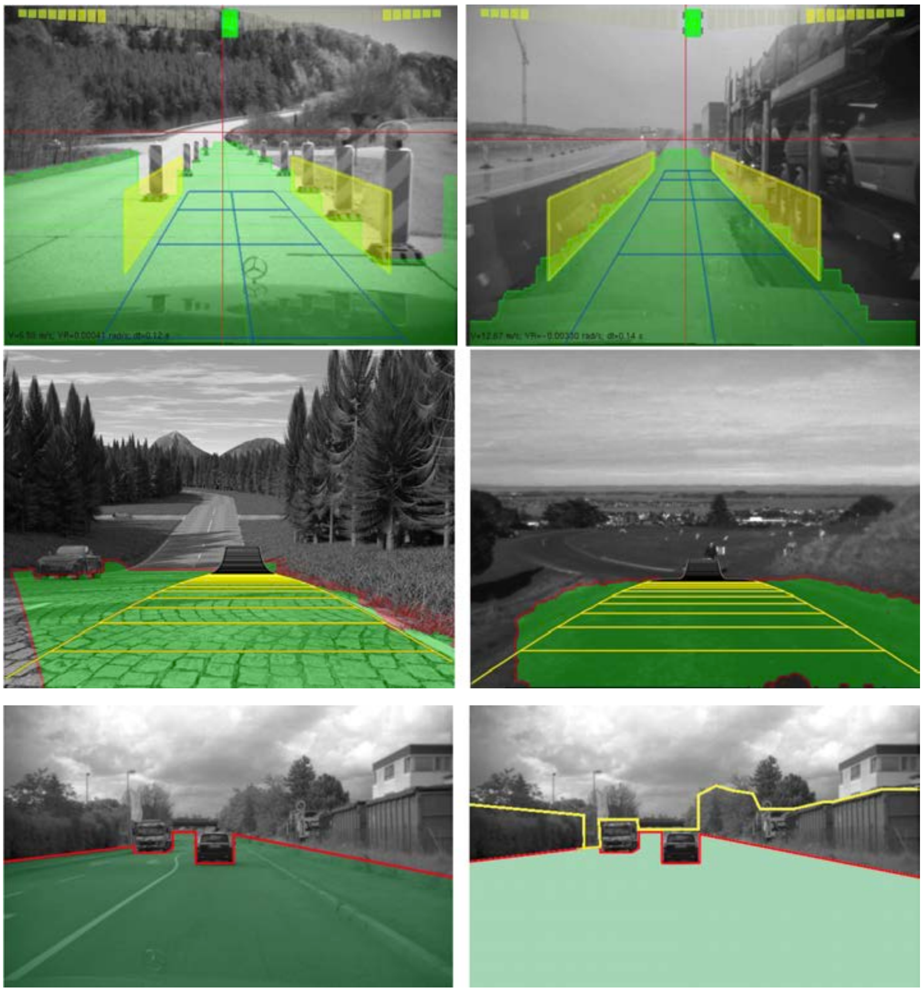

Figure 19: *Top, left*: Results for a highway and a freeway. Courtesy of the authors of [11]. *Top, right*: Road manifold approximation for synthetic and real scene. Courtesy of the authors of [117]. *Bottom*: Free space (right) for the scene shown on the left. Courtesy of the author of [136].

tion, but (bottom of the figure) a vertical road approximation, using a spline representation, supports more accurate free space estimation.

5.2 Higher-order tasks

There is a fluent border between lower and higher order; we consider a task as "higher-order" if more than just one basic task is addressed; higher-order tasks are defined by interaction with other modules in a complex driver assistance system.

5.2.1 Lane-departure and wrong-lane warning

Lane-departure warning (LDW) is an important application of lane detection and tracking systems, especially of value for professional drivers (trucks or long-distance busses). For multi-sensor systems, using cameras and GPS data, see, for example, [29]. Sensor fusion for LDW is discussed in [80, 130], and [59] proposes a fuzzy-rule-based expert system for LDW. Real-time LDW using an FPGA implementation of a specially designed algorithm is the subject of [94].

Driving on the wrong side of the road is addressed by wrong-lane warning systems, which require to understand a multi-lane environment [127].

5.2.2 Detection of driver attentiveness

Driver's attentiveness monitoring is an integrated challenge for autonomous driving and ADAS systems. Understanding the attention level helps to determine when to warn a driver and when to take preventive action. For detecting a driver's attentiveness, complex tasks are necessary to be solved by a comprehensive analysis which classifies attentive and inattentive states, with considering a driver's states, the traffic environment, or other vehicle's moves and states.

[9, 48] utilized an integrate system which combines driver gaze and head pose with road scene features, lane tracking, and traffic signs. [26] reviews a wide range of technologies for driver inattention monitoring, which introduces concepts, measures of inattention, and related commercial products.

5.2.3 Real-view navigation

Real-view navigation is expected to replace navigation based on computer-generated synthetic views. Real video data need to be projected to the driver of the ego-vehicle like being viewed from the current position (e.g. simply recorded if lighting conditions allow to do so), and analysed with respect to the proposed navigation path and the actual lane geometry.

The basic idea presented in [28] (see Figs. 20 and 21) has been implemented for a prototype of a video-based car navigation system developed by the Electronics Telecommunications Research Institute (ETRI). [49] designed a navigation system showing real-view image servicing routes and various other guide information. [1] proposed a navigation system which overlays computer graphics elements on live video captured by the in-vehicle camera.

5.2.4 Head-up display systems

A head-up display (HUD) is a virtual screen which appears in the windshield, displaying indicative information, and guiding the route with graphical components. The driver looks forward without turning head or eyes down to see the provided information, and its position can be controlled by understanding the pose of the driver's head. It is difficult to match the location and direction of lanes with projected virtual objects, and to calculate a driver's head direction and gaze for understanding the viewing angle.

[100] is one of the many publications which present the concept of both AR navigation and HUD system in cars.

See Figs. 22 Recently, high-end cars start to use coloured HUDs to display combined real-view and navigation information. This new technology provides the opportunity to present not only current traffic or road information (e.g. current speed and speed limit, gear position, or fuel gauge) but also directional indicators or attention signs into the correct viewing direction of the driver, aligned with the visible real world. [128] introduces a capable AR-HUD system for installation in a vehicle, and [107] designed an AR-HUD system with object recognition, head tracking and projection of traffic information.

6 Diversity of Scenarios and Evaluation

A *scenario* or *situation* is defined by current road geometry, other traffic participants, or environmental influences, such as traffic events(road intersections, highway exits, or roundabouts, challenging viewing or lighting conditions (e.g. shadows, night, rain with running wipers, snow, or fog), occlusions caused by pedestrians or other closely driving vehicles, moving objects in the traffic scene

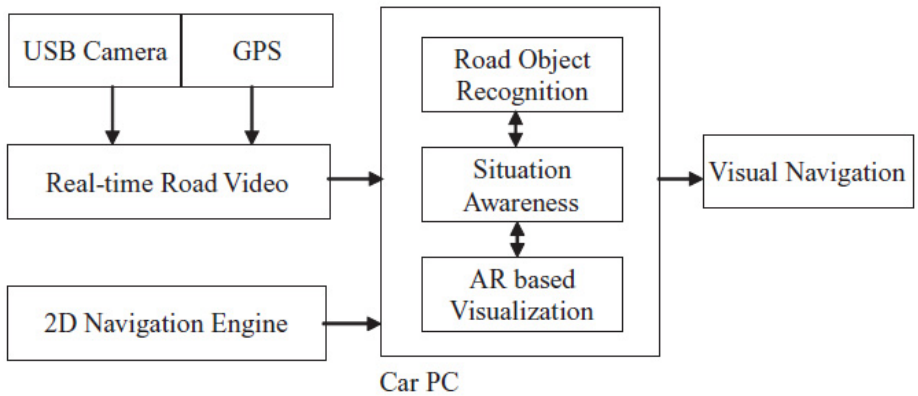

Figure 20: This block diagram shows three modules: a road object recognition module for understanding road features such as lane markings and lane colour, an AR-based visualization module (AR stands for "augmented reality") for superimposing route guidance on a live video, and a situation awareness module for understanding dynamic traffic situations. Courtesy of the authors of [28].

Figure 21: Example of two screenshots for real-view navigation. Courtesy of the authors of [28].

such as trees along the road.

We discuss some challenges depending on scenarios. The section addresses the axis of scenarios in the scope of lane analysis as shown in Fig. 2. Due to rarely existing explicit alignments between scenarios and proposed methods we do not include a summarizing table into this section, as for the previous three sections. This points to a need to address assumed conditions for a proposed method more clearly, already starting with ways how to characterize conditions (scenarios) by statistical or descriptive models. Evaluations based on data provided with ground truth are a step towards such characterizations.

Figure 22: *Left:* a sketch in 2004 pointing to future work on mapping navigation data into the windshield; the yellow line is projected onto a virtual screen for highlighting the road. Understanding of the driver's head pose is needed [100]. Such projections (onto a virtual screen) are reality by now. *Right*: HUD technology appears in cars currently projecting information into windshields or mirrors. Image in the public domain [7].

Table 3: References for tasks and applications.

Applications	Features	References
Road modelling	Detect road surfaces (manifolds), and shape	[91, 117] [118, 124]
Lane markers	Using detected edges and segments. Important for subjects related to road understanding	[5, 12, 22] [23, 27, 89]
Curbs	Considered to be straight or curved driving area delimiters	[105, 106, 121] [122, 139]
Corridor	Understanding of the expected space the ego-vehicle will drive in	[63, 65]
Free space	A region the ego-vehicle can drive in without collision Permanent task for autonomous driving vehicle.	[11, 27, 137] [138, 139]
Lane-departure and wrong-lane warning	Using multi-sensor, camera, GPS data. Warning when vehicle moves out of lane, or drives in wrong lane Understanding of the trajectory of the vehicle	[29, 59, 80] [127, 130]
Driver attentiveness and surround information	Understanding status of driver, traffic and driving environment, including other vehicles	[9, 26, 48]
Real-view navigation	$3^n d$ generation car navigation system, Real view-based services providing realistic and dynamic information	[1, 28, 49]
Head-up display system	Presenting current traffic or road information, guiding a route with graphical components. Head tracking, projecting a corresponding view with traffic information.	[100, 107, 128]

6.1 Difficulties and challenges

Difficulties are caused by challenges in scenarios, difficulties can also occur if a used model does not match sufficiently with the real-world (e.g. left and right lane borders not parallel, do not match a simplified geometric curve model such as, for example, parabolic lane borders). Difficulties are also caused if used methodologies are not fully understood, applied under the wrong circumstances, or just to simple to be able to deal with the complexity of the real world.

It is expected that vision-based driver assistance has to include mechanisms for adapting applied computer vision techniques to the current scenario [73]; see Figure 24. For analysing the performance of techniques on scenarios, those need to be represented, e.g. by statistical properties of video data measures [125]. The paper [62] details particular challenges for lane detectors by means of examples and informal descriptions of scenarios. Future research might generalise such descriptions by using, e.g., data measures as suggested in [125] and further developed in [120].

6.2 Discussion of adverse conditions

A simple scenario is, for example, given by clearly marked lanes on a highway, sparse traffic, and bright daylight without any disturbing events such as a sun strike. Basically, edge detection followed by the standard Hough transform (for detecting straight lines) solves the lane detection problem for such a simple scenario, and thus already very much for daytime driving on a highway. However, with variations from a simple scenario, the complexity of the lane detection task may increase considerably.

6.2.1 Lighting and weather conditions

Lane detection at night is a special challenge [20]. [21] applies a linear lane model for such situations. [20] also discuss ground truth generation for night-time lane detection.

[47] deals with lighting variations, particularly shadows, and such techniques have been applied in [3, 4, 38]. See Fig. 23 for an example of processing images for removing shadows. The removal of shadows in the grey-level image can be achieved in real time; a final (but not necessary for lane detection) colour conversion into a shadow-reduced colour image would be time consuming. The method requires that image data are recorded in three different narrow bands such as red, green, and blue. Weather conditions have been studied in [52], proposing the use of optic flow detection for lane recognition. [88] also discusses situations showing heavy rain. The presence of windscreen wiper movement is discussed in [118].

6.2.2 Multi-lane conditions

The detection of multiple lanes is considered in [10, 84, 127]. Authors assume either lane markings [16], or scenarios without lane markings [135]. Overtaking assistance also requires to understand adjacent lanes on a road. Multiple lane detection based on multi-object Bayes filtering is presented in [35]. Driving on a freeway has been discussed in [37, 78], and on urban roads in [119].

6.2.3 Traffic and occlusion conditions

The understanding of lanes at road intersections or roundabouts defines a particular challenge which requires more research into this subject. Long-distance lane perception, rather than just short-distance detection, is addressed in [88]. The implementation of lane detection on mobile phones is discussed in [111], using monocular vision (i.e. of the single integrated camera) only. [82] deals with the occlusion caused by a close leading vehicle.

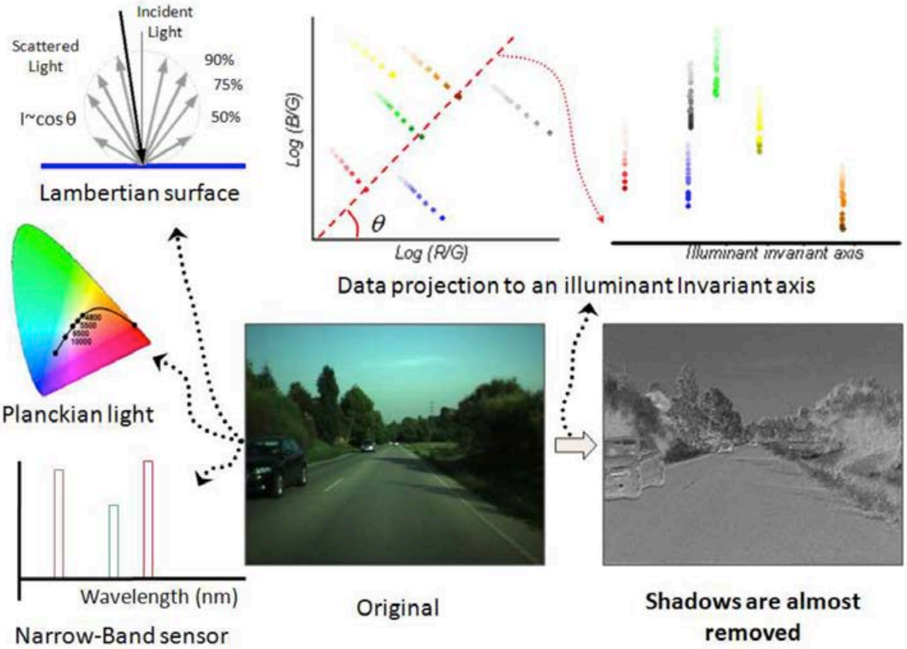

Figure 23: An illumination-invariant image can be obtained under the assumptions of Planckian light, Lambertian surfaces, and narrowband sensors (illustrated on the left). A colour-conversion (not illustrated here) can then map an original image into an almost shadow free image. Courtesy of the authors of [3].

6.3 Performance evaluation

Typically, papers proposing a novel technique in the context of vision-based lane analysis also provide some experimental results about accuracy (for selected scenarios) or robustness (i.e. accuracy across a selection of different scenarios, preferably also including challenging scenarios). For example, [115] provides a detailed discussion about robustness of an embedded solution for lane analysis.

6.3.1 Comparative evaluation

Some papers contain a comparative analysis with another technique suggested (by others) for the same task. By not having original sources (of the other authors) at hand limits the meaningfulness of such comparisons. Comparing results of different techniques on the same input data is a good compromise.

There is still no benchmark dataset of “reasonable complexity” available which provides “reasonable ground truth” for lane-analysis tasks (for example, comparable to the complexity of existing video data bases for stereo analysis

Figure 24: Eight different scenarios, called *barriers*, *dusk*, *harbour bridge*, *midday*, *night*, *people*, *Queen Street*, and *wiper*, of Set 9 of EISATS (see text for a link to this website). Lane detection is of varying difficulty depending on the given scenario.

or optic flow calculation with provided ground truth, such as on KITTI[6] or EISATS). However, KITTI started with providing 289 frames with manually labelled road or lane areas. A larger data set is in preparation for EISATS [2]; see also Fig. 26.

Comparative performance evaluation also has its limitations; there is no linear order of techniques with respect to all kinds of scenarios. Typically, techniques come with their particular benefits or drawbacks, to be discussed carefully in dependency of scenarios. An adaptive selection of techniques and parameters appears to be a general key for optimisation.

6.3.2 Example: Comparison of three lane-detectors

For a detailed comparative discussion of three different lane detectors, proposed in [5, 64, 119], see [62]. Examples 6 and 7 above detail the detector defined in [64].

The paper [62] analyses particular challenges for lane detectors by means of examples and informal descriptions of scenarios, and uses then the same test data for comparing the three lane detectors. The test data used contains four colour clips (1,224 frames in total) recorded in a vehicle, provided by [5], together with a MATLAB tool for manually labelling lane marks as ground truth (a time-consuming process).

There is no simplistic conclusion about a linear order in [62] for the compared three methods. For the considered diversity of scenarios, there are tables, diagrams, figures showing examples of results (Fig. 25 is one of those), and various discussions about particular benefits or drawbacks of the compared methods.

6.3.3 Generation of lane-border ground truth

Despite having many algorithms and approaches available for vision-based lane analysis, an ongoing concern [14, 95] is the lack of proper ground-truth estimation to evaluate efficiencies and accuracies.

Simulated ground truth was created in [112]. After adapting a lane detection algorithm to this synthetic ground truth, it did not work very well on real data. The conclusion was that there is a need for another way of ground-truth generation.

For a semi-automatic technique using time slices and splines to generate ground truth from a road image sequence, see [17, 19, 20]. The proposed approach works reasonably well on clearly marked roads, but the involved interaction also comes with the risk of human error and limited usability. It appears that the proposed approach can be improved further for reducing required human interactions. Figure 26 illustrates results of generated ground truth when applying two different techniques, using input data provided by [19].

[6] Vision benchmark suite of the Karlsruhe Institute of Technology and the Toyota Technological Institute at Chicago; see www.cvlibs.net/datasets/kitti/.

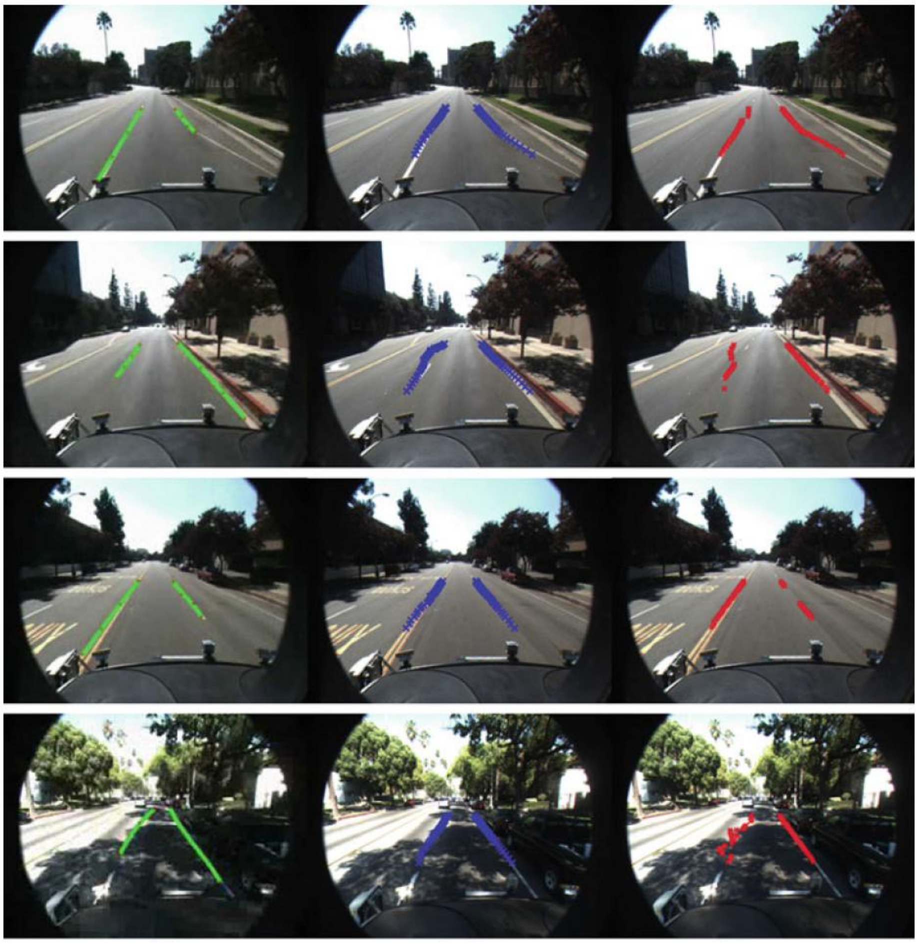

Figure 25: Lane detection results for three different algorithms. *Left*: Lane detection following [5]. *Middle*: Lane detection following [64]. *Right* Lane detection following [119]. Courtesy of the authors of [62].

7 Conclusions

There is already a wide variety in proposed methods for lane analysis; the given references below only represent a small percentage of publications in this area. Besides, this work typically still focuses on individual components. Therefore, this survey aimed at presenting developments in *visual lane analysis* towards integrated systems combining multiple processes for one defined goal. We provided basic definitions, and illustrated models and potential methods by giving details and examples by using independent axes.

This is one of the differences of our review to previous summarizing publica-

Figure 26: Generated ground-truth lane borders. *Left*: With the original interactive approach of [17]. *Right*: Generated ground truth when using an automatic edge-operator-based approach. Courtesy of the authors of [2].

tions in the field, and we also differ by lists of discussed subjects (and by being a little more recent).

The success (measured in efficiency and robustness) of lane analysis methods depends on the given scenario. Adaptation to scenarios appears to be a logical consequence; there is no all-time-winner, detection and tracking methods should be configured or selected (out of a *tool box*) in real time while driving. Statistical image features, or results derived from various vision modules (e.g. for stereo and motion analysis) for previous image frames at times $< t+1$ might be tested for possible guidance of such an adaptation process.

Acknowledgements. We thank all the colleagues who gave their permissions for the inclusion of their figures into this survey. We also thank Ali Al-Sarraf, Mahdi Rezaei, and Junli Tao, members of the *.enpeda..* group, The University of Auckland, for help in collecting references and related discussions.

References

[1] K. Akaho, T. Nakagawa, Y. Yamaguchi, K. Kawai, H. Kato, and S. Nishida, "A study and evaluation on route guidance of a car navigation system based on augmented reality", in *Human-Computer Interaction* (J.A. Jacko, editor), LNCS 6763, pages 357–366, 2011

[2] A. Al Sarraf, B.-S. Shin, Z. Xu, and R. Klette, "Ground truth and performance evaluation
of lane border detection", Technical Report, MItech-TR 85, The University of Auckland, 2013

[3] J.M. Álvarez, A.M. López, and R. Baldrich, "Illuminant invariant model-based road segmentation", in Proc. *IEEE Intelligent Vehicle Symp.*, 2008

[4] J.M. Álvarez and A.M. López, "Road detection based on illuminant invariance," *IEEE Trans. Intelligent Transportation Systems*, **12**:1524–90520, 2011

[5] M. Aly, "Real time detection of lane markers in urban streets", in Proc. *IEEE Intelligent Vehicle Symp.*, pages 7–12, 2008

[6] Anonymous, "Richtlinien für die Markierung von Strassen, RMS", Forschungsgesellschaft für das Strassenwesen, 1980

[7] Anonymous, "Holographic heads-up display for car mirrors", www.telovation.com/articles/holographic-heads-display-car-mirrors.html, 2009

[8] N. Apostoloff and A. Zelinsky, "Robust vision based lane tracking using multiple cues and particle filtering", in Proc. *IEEE Intelligent Vehicles Symposium*, pages 558–563, 2003

[9] N. Apostoloff and A. Zelinsky, "Vision in and out of vehicles: Integrated driver and road scene monitoring", *The Int. J. Robotics Research*, **28**:774–801, 2009

[10] R. Aufrére, R. Chapuis, and F. Chausse, "A model-driven approach for real-time road recognition", *Machine Vision Applications*, **13**:95–107, 2001

[11] H. Badino, U. Franke, and R. Mester, "Free space computation using stochastic occupancy grids and dynamic programming", in Proc. *ICCV Workshop Dynamical Vision*, 2007

[12] J.H. Bae and J.B. Song. "Monocular vision-based lane detection using segmented regions from edge information", in Proc. *URAI*, pages 499–502

[13] D.H. Ballard, "Generalizing the Hough transform to detect arbitrary shapes", *Pattern Recognition*,**13**:111–122, 1981

[14] A. Bar Hillel, R. Lerner, D. Levi, and G. Raz, "Recent progress in road and lane detection: a survey," *Machine Vision Applications*, **23**, 19 pages, 2012

[15] M. Bellino, Y.L. de Meneses, P. Ryser, and J. Jacot, "Lane detection algorithm for an onboard camera", in SPIE Proc. 5663, *Photonics Automobile*, pages 102–111, 2005

[16] M. Bertozzi and A. Broggi, "GOLD - A parallel real-time stereo vision system for generic obstacle and lane detection", *IEEE Trans. Image Processing*, **7**:62–81, 1998

[17] A. Borkar, "Multi-viewpoint lane detection with applications in driver safety systems", PhD thesis, Georgia Institute of Technology, 2012

[18] A. Borkar, M. Hayes, M.T. Smith, "Lane detection and tracking using a layered approach", in Proc. *Advanced Concepts Intelligent Vision Systems*, LNCS 5807, pages 474–484, 2009

[19] A. Borkar, M. Hayes, M.T. Smith, "An efficient method to generate ground truth for evaluating lane detection systems", In Proc. *IEEE Int. Conf. Acoustics Speech Signal Processing*, pages 1090–1093, 2010

[20] A. Borkar, M. Hayes, and M. T. Smith, "A novel lane detection system with efficient ground truth generation", *IEEE Trans. Intelligent Transportation Systems*, **13**:365–374, 2012

[21] A. Borkar, M. Hayes, M. T. Smith, and S. Pankanti, "A layered approach to robust lane detection at night", in Proc. *Computational Intelligence Vehicles Vehicular Systems*, pages 51–57, 2009

[22] J. Byun, K.I. Na, M. Noh, and S. Kim, "ESTRO: Design and development of intelligent autonomous vehicle for shuttle service in the ETRI ", in Proc. *Workshop Planning Perception Navigation Intelligent Vehicles*, Portugal, 2012

[23] P. Boyraz, X. Yang, and J.H.L. Hansen, "Computer vision systems for 'context-aware' active vehicle safety and driver assistance", in *Digital Signal Processing for In-Vehicle Systems and Safety* (J.H.L. Hansen, ed.), pages 217–227, Springer, 2012

[24] A. Broggi, "Robust real-time lane and road detection in critical shadow conditions", in Proc. *IEEE Intelligent Vehicle Symp.*, pages 353–358, 1995

[25] Y. Chen, M. He, and Y. Zhang, "Robust lane detection based on gradient direction", in Proc. *IEEE Int. Conf. Industrial Electronics Applications*, pages 1547–1552, 2011

[26] Y. Dong, Z. Hu, K. Uchimura, and N. Murayama, "Driver inattention monitoring system for intelligent vehicles: A review", *IEEE Trans. Intelligent Transportation Systems*, **12**:596–614, 2011

[27] J. Choi, J. Lee, D. Kim, G. Soprani, P. Cerri, A. Broggi, and K. Yi, "Environment-detection-and-mapping algorithm for autonomous driving in rural or off-road environment", *IEEE Trans. Intelligent Transportation Systems*, **13**:974–982, 2012

[28] K.-H. Choi, S.-Y. Park, S.-H. Kim, K.-S. Lee, J.-H. Park, S.-I. Cho, and J.-H. Park, "Methods to detect road features for video-based in-vehicle navigation systems", *J. Intelligent Transportation Systems: Technology Planning Operations*, **14**:13–26, 2010

[29] J.M. Clanton, D.M. Bevly, and A. Scottedward Hodel, "A low-cost solution for integrated multisensor lane departure warning system", *IEEE Trans. Intelligent Transportation Systems*, **10**:47–59, 2009

[30] J.D. Crisman and C.E. Thorpe, "SCARF: A colour vision system that tracks roads and intersections", *IEEE Trans. Robotics Automation*, **9**:49–58, 1993

[31] R. Dahyot, "Statistical Hough transform", *IEEE Trans. Pattern Analysis Machine Intelligence*, **31**:1502–1509, 2009

[32] R. Danescu, S. Nedevschi, M.M. Meinecke, and T.B. To, "Lane geometry estimation in urban environments using a stereo vision system", in Proc. *Int. Conf. Intelligent Transportation Systems*, pages 271–276, 2007

[33] R. Danescu and S. Nedevschi, "Probabilistic lane tracking in difficult road scenarios using stereovision", *IEEE Trans. Intelligent Transportation Systems*, **10**:272–282, 2009

[34] R. Danescu and S. Nedevschi, "New results in stereovision based lane tracking," in Proc. *IEEE Intelligent Vehicles Symposium*, pages 230–235, 2011

[35] H. Deusch, J. Wiest, S. Reuter, M. Szczot, M. Konrad, and K. Dietmayer, "A random finite set approach to multiple lane detection", in Proc. *Int. IEEE Conf. Intelligent Transportation Systems*, pages 270–275, 2012

[36] E.D. Dickmanns, "*Dynamic Vision for Perception and Control of Motion*", Springer, London, 2007

[37] E.D. Dickmanns and B.D. Mysliwetz, "Recursive 3-D road and relative ego-state recognition", *IEEE Trans. Pattern Recognition Machine Intelligence*, **14**:199–213, 1992

[38] F. Dornaika, J.M. Álvarez, A.D. Sappa, and A.M. López, "A new framework for stereo sensor pose through road segmentation and registration", *IEEE Trans. Intelligent Transportation Systems*, **12**:954–966, 2011

[39] R.O. Duda and P. E. Hart, "Use of the Hough transformation to detect lines and curves in pictures", *Comm. ACM*, **15**:11—15, 1972

[40] O. Ecabert and J.P. Thiran, "Adaptive Hough transform for the detection of natural shapes under weak affine transformations", *Pattern Recognition*, **25**:1411–1419, 2004

[41] A. Eidehall and F. Gustafsson, "Combined road prediction and target tracking in collision avoidance", in Proc. *IEEE Intelligent Vehicles Symposium*, pages 619–624, 2004

[42] R. Fabbri, L. Da F. Costa, J.C. Torelli, and O.M. Bruno, "2D Euclidean distance transform algorithms: A comparative survey", *ACM Computing Surveys*, **40**, article no. 2, 2008

[43] C. Fan, L. Hou, S. Di, and J. Xu, "Research on the lane detection algorithm based on zoning Hough transformation", *Advanced Materials Research*, volumes 490–495, pages 1862–1866, 2012

[44] B. Fardi and G. Wanielik, “Hough transformation based approach for road border detection in infrared images”, in Proc. *IEEE Intelligent Vehicles Symposium*, pages 549–554, 2004

[45] P.F. Felzenszwalb and D.P. Huttenlocher, “Distance transform of sampled functions”, Cornell Computing and Information Science, Technical Report TR 2004-1963, 2004

[46] M. Felisa and P. Zani, “Robust monocular lane detection in urban environments”, in Proc. *IEEE Intelligent Vehicle Symposium*, pages 591–596, 2010

[47] G. Finlayson, S. Hordley, C. Lu, and M. Drew, “On the removal of shadows from images”, *IEEE Trans. Pattern Analysis Machine Intelligence*, **28**:59–68, 2006

[48] L. Fletcher and A. Zelinsky, “Driver state monitoring to mitigate distraction”, in Proc. *Int. Conf. Distractions Driving*, Australia, 2007

[49] C. Ga and K. Yu, “Design of real-view navigation system with virtual path mapping technique”, in Proc. *ASPRS/MAPPS*, 2009

[50] C. Gackstatter, S. Thomas, P. Heinemann, and G. Klinke, “Stable road lane model based on clothoids”, in Proc. *Int. Forum Advanced Microsystems Automotive Applications*, 2010

[51] S. Gehrig, F. Eberli, and T. Meyer, “A real-time low-power stereo vision engine using semi-global matching”, In Proc. *Int. Conf. Computer Vision Systems*, LNCS 5815, pages 134–143, 2009

[52] A. Gern, R. Moebus, and U. Franke, “Vision-based lane recognition under adverse weather conditions using optical flow”, in Proc. *IEEE Intelligent Vehicle Symposium*, volume 2, pages 652–657, 2002

[53] S. Guan, R. Klette, and Y.W. Woo, “Belief propagation for stereo analysis of night-vision sequences”, In Proc. *Pacific-Rim Symp. Image Video Technology*, LNCS 5414, pages 932–943, 2009

[54] K. Hashimoto, S. Nakayama, T. Saito, S. Ishida, K. Unuora, J. Ishii, N. Oono, and Y. Okada, “An image processing architecture and a motion control method for an autonomous vehicle”, in Proc. *IEEE Intelligent Vehicles Symposium*, New York , 2002

[55] S. Hermann, A. Boerner, and R. Klette, “Mid-level segmentation and segment tracking for long-range stereo analysis”, In Proc. *Pacific-Rim Symp. Image Video Technology*, LNCS 7087, pages 224-235, Springer, 2011

[56] S. Hermann and R. Klette, “The naked truth about cost functions for stereo matching”, MItech-TR 33, The University of Auckland, 2009

[57] S. Hermann and R. Klette, "Iterative semi-global matching for robust driver assistance systems", In Proc. *Asian Conf. Computer Vision*, LNCS, 2013

[58] H. Hirschmüller, "Accurate and efficient stereo processing by semi-global matching and mutual information", In Proc. *IEEE Int. Conf. Computer Vision Pattern Recognition*, volume 2, pages 807–814, 2005

[59] P.Y. Hsiao, C.W. Yeh, S.S. Huang, and L.C. Fu, "A portable vision-based real-time lane departure warning system: Day and night", *IEEE TRans. Vehicular Technology*, **58**:2089–2094, 2009

[60] M. Isard and A. Blake, "Condensation: conditional density propagation for visual tracking", *Int. J. Computer Vision*, **29**:5–28, 1998

[61] P. Jeong and S. Nedevschi, "Efficient and robust classification method using combined feature vector for lane detection", *IEEE Trans. Circuits Systems Video Technology*, **15**:528–537, 2005

[62] R. Jiang, R. Klette, T. Vaudrey, and S. Wang, "Lane detection and tracking using a new lane model and distance transform", *Machine Vision Applications*, **22**:721–737, 2011

[63] R. Jiang, R. Klette, T. Vaudrey, and S. Wang, "Corridor detection for vision-based driver assistance systems", *Int. J. Pattern Recognition and Artificial Intelligence*, **25**:253–272, 2011

[64] R. Jiang, R. Klette, S. Wang, and T. Vaudrey, "New lane model and distance transform for lane detection and tracking", In Proc. *Computer Analysis Images Patterns*, LNCS 5702, pages 1044-1052, 2009

[65] R. Jiang, R. Klette, S. Wang, and T. Vaudrey, "Ego-vehicle corridors for vision-based driver assistance", In Proc. *IWCIA*, LNCS 5852, pages 238-251, 2009

[66] R. Jiang, M. Terauchi, R. Klette, S. Wang, and T. Vaudrey, "Low-level image processing for lane detection and tracking", In Proc. *ArtsIT*, LNICST 30, pages 190-197, 2009

[67] T.M. Jochem, D.A. Pomerleau, and C.E. Thorpe, "MANIAC: A next generation neurally based autonomous road follower", in Proc. *Int. Conf. Intelligent Autonomous Systems*, pages 473–479, 1993

[68] C.R. Jung and C.R. Kelber, "A lane departure warning system based on a linear-parabolic lane model", in Proc. *IEEE Intelligent Vehicle Symp.*, pages 891–895, 2004

[69] M. Kass, A. Witkin, and D. Terzopoulos, "Snakes: Active contour models," *Int. J. Computer Vision*, **1**:321–331, 1988

[70] Z. Kim, "Realtime lane tracking of curved local road", in Proc. *Int. Conf. Intelligent Transportation Systems*, pages 1149–1155, 2006

[71] Z. Kim, "Robust lane detection and tracking in challenging scenarios", *IEEE Trans. Intelligent Transportation Systems*, **9**:16–26, 2008

[72] R. Klette, "Concise Computer Vision", Springer, London (UK), January 2014

[73] R. Klette, S. Morales, T. Vaudrey, J. Morris, C. Rabe, and R. Haeusler, "Stereo and motion analysis of long stereo image sequences for vision-based driver assistance", keynote at *DAGM 2009*, Jena University, 2009

[74] R. Klette and A. Rosenfeld, "Digital Geometry", Morgan Kaufmann, San Francisco, 2004

[75] R.E.J. Kneepkens, "Hough-based road detection", Master thesis, TU Eindhoven, 2005

[76] C. Kreucher and S. Lakshmanan, "LANA: A lane extraction algorithm that uses frequency domain features" *IEEE Trans. Robotics Automation*, **15**:343–350, 1999

[77] C. Kreucher and S. Lakshmanan, "A frequency domain approach to lane detection in roadway images", in Proc. *Int. Conf. Image Processing*, pages 31–35, 1999

[78] D. Khosla, "Accurate estimation of forward path geometry using two-clothoid road model", in Proc. *IEEE Intelligent Vehicle Symp.*, volume 1, pages 154–159, 2002

[79] R. Labayrade, D. Aubert, and J.-P. Tarel, "Real-time obstacle detection in stereovision on non flat road geometry through 'v-disparity' representation", In Proc. *Symposium Intelligent Vehicles*, pages 646–651, 2002

[80] J.W. Lee and J.S. Cho, "Effective lane detection and tracking method using statistical modelling of colour and lane edge-orientation", in Proc. *IEEE Int. Conf. Computer Sciences Convergence IT*, pages 1586–1591, 2009

[81] S. Lee and W. Kwon, "Robust lane keeping from novel sensor fusion", in Proc. *IEEE Int. Conf. Robotics and Automation*, volume 4, pages 3704–3709, 2001

[82] H. Li and F. Nashashibi, "Robust real-time lane detection based on lane mark segment features and general a priori knowledge", in Proc. *IEEE Int. Conf. Robotics Biometrics*, pages 812–817, 2011

[83] Q. Li, N. Zheng, and H. Cheng, "Springrobot: A prototype autonomous vehicle and its algorithms for lane detection", *IEEE Trans. Intelligent Transportation Systems*, **5**:300–308, 2004

[84] C. Lipski, B. Scholz, B. Berger, C. Linz, and T. Stich, "A fast and robust approach to lane marking detection and lane tracking", in Proc. *IEEE Southwest Symp. Image Analysis Interpretation*, pages 57–60, 2008

[85] G. Liu, F. Worgotter, and I. Markelie, "Lane shape estimation using a partitioned particle filter for autonomous driving", in Proc. IEEE Int. Conf. Robotics Automation, pages 1627–1633, 2011

[86] G. Liu, F. Worgotter, and I. Markelie, "Combining statistical Hough transform and particle filter for robust lane detection and tracking", in Proc. *IEEE Intelligent Vehicle Symposium*, pages 993–997, 2010

[87] W. Liu, H. Zhang, B. Duan, H. Yuan, and H. Zhao, "Vision-based realtime lane marking detection and tracking", in Proc. *IEEE Int. Conf. Intelligent Transportation Systems*, pages 49–54, 2008

[88] X. Liu, X. Xu, and B. Dai, "Vision-based long-distance lane perception and front vehicle location for autonomous vehicles on highway roads", *J. Cent. South. Univ.*, **19**:1454–1465, 2012

[89] X. Liu, G. Wang, J. Liao, B. Li, Q. He, and M.Q.H. Meng, "Detection of geometric shape for traffic lane and mark", in Proc. *IEEE Int. Conf. Information Automation*, pages 395–399, 2012

[90] H. Loose and U. Franke, "Kalman particle filter for lane recognition on rural roads", in Proc. *IEEE Intelligent Vehicles Symposium*, 2009

[91] H. Loose and U. Franke, "B-spline based road model for 3D lane recognition", in Proc. *ITSC*, 2010

[92] A. M. López, J. Serrat, C. Cañero, F. Lumbreras, and T. Graf, "Robust lane markings detection and road geometry computation", *Int. J. Automotive Technology*, **11**:395–407, 2010

[93] Q.T. Luong, J. Weber, D. Koller, and J. Malik, "An integrated stereo-based approach to automatic vehicle guidance", in Proc. *Int. Conf. Computer Vision*, pages 52–57, 2002

[94] R. Marzotto, P. Zoratti, D. Bagni, A. Colombari, and V. Murino, "A realtime versatile roadway path extraction and tracking on an FPGA platform", *Computer Vision Image Understanding*, **114**:1164–1179, 2010

[95] J.C. McCall and M.M. Trivedi, "Video-based lane estimation and tracking for driver assistance: Survey, system, and evaluation", *IEEE Trans. Intelligent Transportation Systems*, **7**:20–37, 2006

[96] J. McDonald, "Detecting and tracking road markings using the Hough transform", in Proc. *the Irish Machine Vision and Image Processing*, 2001

[97] M. Meuter, S. Müller-Schneiders, A. Mika, S. Hold, C. Nunn, and A. Kummert, "A novel approach to lane detection and tracking", in Proc. *IEEE Int. Conf. Intelligent Transportation Systems*, pages 1–6, 2009

[98] S. Morales and R. Klette, "Ground truth evaluation of stereo algorithms for real world applications", In Proc. *CVVT*, LNCS 6469, pages 152-162, ACCV workshop, 2011

[99] A.M. Muad, A. Hussain, and S.A. Samad, "Implementation of inverse perspective mapping algorithm for the development of an automatic lane tracking system", in Proc. IEEE TENCON, pages 207–210, 2004

[100] W. Narzt, G. Pomberger, A. Ferscha, D. Kolb, R. Muller, J. Wieghardt, H. Hortner, and C. Lindinger, "A new visualization concept for navigation systems," LNCS 3196, pages 440–451, 2004

[101] M.A. Nasirudin and M.R. Arshad, "A feature-based lane detection system using Hough transform method", in Proc. *Seminar Intelligent Technology Applications*, 4 pages, 2007

[102] S. Nedevschi, F. Oniga, R. Danescu, T. Graf, and R. Schmidt, "Increased accuracy stereo approach for 3D lane detection," in Proc. *IEEE Intelligent Vehicles Symposium*, pages 42–49, 2006

[103] S. Nedevschi, R. Schmidt, T. Graf, R. Danescu, D. Frentiu, T. Marita, F. Oniga, and C. Pocol, "3D lane detection system based on stereovision", in Proc. *Int. Conf. Intelligent Transportation Systems*, pages 161–166, 2004

[104] M. Nieto, L. Salgado, F. Jaureguizar, and J. Arrospide, "Robust multiple lane road modelling based on perspective analysis", in Proc. *IEEE Int. Conf. Image Processing*, pages 2396–2399, 2008

[105] F. Oniga and S. Nedevschi, "Polynomial curb detection based on dense stereovision for driving assistance", in Proc. *Int. IEEE Conf. Intelligent Transportation Systems*, pages 1110–1115, 2010

[106] F. Oniga, S. Nedevschi, and M.M. Meinecke, "Curb detection based on a multi-frame persistence map for urban driving scenarios", in Proc. *Int. IEEE Conf. Intelligent Transportation Systems*, pages 67–72, 2008

[107] H. Park and K.-H. Kim, "Efficient information representation method for driver-centered AR-HUD system", in Proc. *User Experience Novel Technological Environments*, LNCS 8014, pages 393–400, 2013

[108] R. Pepy, A. Lambert, and H. Mounier, "Path planning using a dynamic vehicle model", in Proc. *IEEE Conf. Information Communication Technologies*, pages 781–786, 2006

[109] D. Pomerleau, "RALPH: Rapidly adapting lateral position handler", in Proc. *IEEE Intelligent Vehicle Symp.*, pages 506–511, 1995

[110] J. Radon, "Über die Bestimmung von Funktionen durch ihre Integralwerte längs gewisser Mannigfaltigkeiten", *Berichte Verhandlungen Königlich-Sächsischen Akademie der Wissenschaften zu Leipzig, Mathematisch-Physische Klasse*, **69**:262–277, 1917

[111] F. Ren, J. Huang, M. Terauchi, R. Jiang, and R. Klette, "Lane detection on the iPhone", in Proc. *ArtsIT*, LNICST 30, pages 198-205, 2009

[112] M. Revilloud, D. Gruyer, and E. Pollard, "Generator of road marking textures and associated ground truth applied to the evaluation of road marking detection", In Proc. *IEEE Int. Conf. Intelligent Transportation Systems*, pages 933 – 938, 2012

[113] M. Rezaei and R. Klette, "Simultaneous analysis of driver behaviour and road condition for driver distraction detection", *Int. J. Image Data Fusion* **2**:217-236, 2011

[114] R. K. Satzoda, S. Sathyanarayana, T. Srikanthan, and S. Sathyanarayana, "Hierarchical additive Hough transform for lane detection", *IEEE Embedded Systems Letters*, **2**(2):23–26, 2010

[115] R. K. Satzoda and M. M. Trivedi, "Vision-based lane analysis: Exploration of issues and approaches for embedded realization", in Proc. *IEEE Computer Vision Pattern Recognition Workshops*, 2013

[116] A. Saudi, J. Teo, M.H.A. Hijazi, and J. Sulaiman, "Fast lane detection with randomized Hough transform", in Proc. *Int. Symposium Information Technology*, volume 4, pages 1-5, 2008

[117] K. Schauwecker and R. Klette, "A comparative study of two vertical road modelling techniques", In Proc. *CVVT*, LNCS 6469, pages 174-183, ACCV workshop, 2011

[118] K. Schauwecker, S. Morales, S. Hermann, and R. Klette, "A comparative study of stereo-matching algorithms for road-modelling in the presence of windscreen wipers", In Proc. *IEEE Intelligent Vehicles Symposium*, pages 7-12, 2011

[119] S. Sehestedt, S. Kodagoda, A. Alempijevic, and G. Dissanayake, "Efficient lane detection and tracking in urban environments", in Proc. *European Conf. Mobile Robots*, pages 126–131, 2007

[120] B.-S. Shin, D. Caudillo, and R. Klette. "Evaluation of two stereo matchers on long real-world video sequences", *Pattern Recognition* (to appear, 2014)

[121] J. Siegemund, U. Franke, W. Förstner, "A temporal filter approach for detection and reconstruction of curbs and road surfaces based on conditional random fields", in Proc. *IEEE Intelligent Vehicles Symposium*, 2011

[122] J. Siegemund, D. Pfeiffer, U. Franke, and W. Förstner, "Curb reconstruction using conditional random fields", in Proc. *IEEE Intelligent Vehicles Symposium*, pages 203–2010, 2010

[123] S. Sivaraman and M. M. Trivedi, "Integrated lane and vehicle detection, localization, and tracking: A synergistic approach", *IEEE Trans. Intelligent Transportation Systems*, **14**:906–917, 2013

[124] B. Southall and C. Taylor, "Stochastic road shape estimation", in Proc. *Int. Conf. Computer Vision*, volume 1, pages 205–212, 2001

[125] V. Suaste, D. Caudillo, B. Shin, and R. Klette, "Third-eye stereo analysis evaluation enhanced by data measures", in Proc. *Mexican Conf. Pattern Recognition*, LNCS 7914, pages 74–83, 2013

[126] S. Taheri, "An investigation and design of slip control braking systems integrated with four wheel steering", Ph.D. dissertation, Clemson University, 1990

[127] J. Tao, B. Shin, and R. Klette, "Wrong roadway detection for multi-lane roads", in Proc. *Computer Analysis Images Patterns*, LNCS 8048, pages 50–58, 2013

[128] O. Utsuboya, T. Shimizu, and A. Kurosawa, "Augmented reality head up display for car navigation system", *SID Symp. Digest Technical Papers*, volume 44, Blackwell Publishing Ltd, 2013

[129] T. Vaudrey, S. Morales, A. Wedel, and R. Klette, "Generalized residual image s' effect on illumination artefact removal for correspondence algorithms", *Pattern Recognition*, **44**:2034–2046, 2010

[130] J.-G. Wang, C.-J. Lin, and S.-M. Chen, "Applying fuzzy method to vision-based lane detection and departure warning system", *Expert Systems Applications*, **37**:113–126, 2010

[131] J. Wang, Y. Wu, Z. Liang, and Y. Xi, "Lane detection based on random Hough transform on region of interesting", in Proc. *IEEE Int. Conf. Information Automation*, pages 1735–1740, 2010

[132] Y. Wang, L. Bai, and M. Fairhurst, "Robust road modelling and tracking using condensation", *IEEE Trans. Intelligent Transportation Systems*, **9**:570–579, 2008

[133] Y. Wang, D. Shen, and E.K. Teoh, "Lane detection using Catmull-Rom spline", in Proc. *IEEE Intelligent Vehicle Symposium*, pages 51–57, 1998

[134] Y. Wang and E.K. Teoh, "Object contour extraction using adaptive B-snake model," *J. Mathematical Imaging Vision*, **24**:295–306, 2006

[135] Y. Wang, E.K. Teoh, and D. Shen, "Lane detection and tracking using B-Snake", *Image Vision Computing*, **22**:269–280, 2004

[136] A. Wedel, "3D motion analysis via energy minimization," PhD thesis, Rheinische Friedrich-Wilhelms-Universität Bonn, 2009

[137] A. Wedel, H. Badino, C. Rabe, H. Loose, U. Franke, and D. Cremers, "B-spline modelling of road surfaces with an application to free space estimation", *IEEE Trans. Intelligent Transportation Systems*, 2009

[138] A. Wedel, U. Franke, H. Badino, and D. Cremers, "B-spline modelling of road surfaces with an application to free space estimation", in Proc. *IEEE Intelligent Vehicle Symp.*, pages 828–833, 2008

[139] W.S. Wijesoma, K.R.S. Kodagoda, and A.P. Balasuriya, "Road-boundary detection and tracking using ladar sensing", *IEEE Trans. Robotics Automation*, **20**:456–464, 2004

[140] B.F. Wu, C.T. Lin, and Y.L. Chen, "Dynamic calibration and occlusion handling algorithms for lane tracking", *IEEE TRans. Industrial Electronics*, **56**:1757–1773, 2009

[141] T. Wu, X.Q. Ding, S.J. Wang, and K.Q. Wang, "Video object tracking using improved chamfer matching and condensation particle filter", in SPIE Proc. 6813, *Machine Vision Applications*, 4 pages, 2008

[142] Z. Xu and B. Shin, "A Statistical Method for Peak Localization in Hough Space", in Proc. *Pacific-Rim Symp. Image Video Technology*, LNCS, 2013

[143] Z. Xu and B. Shin, "Accurate Line Segment Detection with Hough Transform Based on Minimum Entropy", in Proc. *Pacific-Rim Symp. Image Video Technology*, LNCS, 2013

[144] Y. Yagi, M. Brady, Y. Kawasaki, and M. Yachida, "Active contour road model for smart vehicle", in Proc. *Int. Conf. Pattern Recognition*, volume 3, pages 3819–3822, 2000

[145] K. Yamaguchi, A. Watanabe, T. Naito, and Y. Ninomiya, "Road region estimation using a sequence of monocular images", in Proc. *Int. Conf. Pattern Recognition*, pages 1–4, 2008

[146] X. Youchun, W. Rongben, and J. Shouwen, "A vision navigation algorithm based on linear lane model", in Proc. *IEEE Intelligent Vehicles Symposium*, pages 240–245, 2000

[147] B. Yu and A.K. Jain, "Lane boundary detection using a multiresolution Hough transform", in Proc. *the IEEE International Conference on Image Processing*, 2002

[148] K. Zhao, M. Meuter, C. Nunn, D. Muller, S. Muller-Schneiders, and J. Pauli, "A novel multi-lane detection and tracking system", in Proc. *IEEE Intelligent Vehicles Symposium*, pages 1084–1089, 2012

[149] Y. Zhou, R. Xu, X. Hu, and Q. Ye, "A robust lane detection and tracking method based on computer vision", *Measurement Science Technology*, **17**:736–745, 2006

[150] S. Zhou, Y. Jiang, J. Xi, J. Gong, G. Xiong, and H. Chen, "A novel lane detection based on geometrical model and Gabor filter", in Proc. *IEEE Intelligent Vehicles Symposium*, pages 59–64, 2010

List of Acronyms

ACC Adaptive cruise control
AR Augmented reality
BPM Belief-propagation matching
DA Driver assistance
DEM Digital elevation map
DT Distance transform
ECCV European Conf. Computer Vision
EDT Euclidean distance transform
EISATS enpeda image sequence analysis test site
enpeda Environment perception and driver assistance
ETRI Electronics Telecommunications Research Institute
GCM Graph-cut matching
GPS Global positioning system
HT Hough transform
HCI Heidelberg Collaboratory for Image Processing
HUD Head-up display
IHC Intelligent headlight control
IPM Inverse perspective mapping
iSGM Iterative SGM
KITTI Karlsruhe Institute Technology & Toyota Institute
LCW Lane change warning
LDW Lane departure warning
LIDAR Light detection and ranging
MCLDW Multi-camera lane departure warning
ODT Orientation distance transform
PDF Point-distribution function
RANSAC Random sample consensus
RODT Row component of ODT
ROI Region of interest
SGM Semi-global matching
SHT Statistical Hough transform
SLAM Simultaneous localization and mapping